Mass-transport and slope accommodation: implications for turbidite sandstone reservoirs

Ben Kneller[1], Mason Dykstra[2], Luke Fairweather[1,3] and Juan Pablo Milana[4]

[1]Department of Geology and Petroleum Geology, University of Aberdeen, Aberdeen AB24 3UE, UK

[2] Statoil Gulf Services, 6300 Bridge Point Parkway, Building 2, Suite 500, Austin, Texas, 78730 USA

[4] Present address: Dana Petroleum, 62 Huntly St, Aberdeen AB10 1RS, UK

[4] Faculdad de Ciencias Exactas, Fisicas y Naturales, Universidad Nacional de San Juan, San Juan, Argentina.

Abstract

Mass transport events are virtually ubiquitous on the modern continental slope, and are also frequent in the stratigraphic record. They are commonly very large (volumes $>10^3$ km^3, areas $>10^4$ km^2, thicknesses $>10^2$ m). They extensively re-mould sea-floor topography on the continental slope and rise. Turbidity currents are highly sensitive to topography, thus turbidite reservoir distribution and geometry can be significantly affected by subjacent mass transport deposits or their slide scars. Given the abundance of mass transport deposits, we should expect that many turbidite systems are so affected. In fact several well-known deepwater outcrops may represent examples of MTD-influenced sedimentation. Turbidites may be captured within slide scars and on the trailing edges of MTDs. They may also be ponded on and around mass transport deposits, in accommodation developed when the mass movement comes to rest, or subsequently due to compaction or creep. The filling of such accommodation depends on the properties of the turbidity currents, their depositional gradient, and how they interact with basin floor topography. The scale of supra-MTD accommodation is determined largely by dynamics of the initial mass flow and internal structure of the final deposit, and typically has a limited range of length scales. We discuss the implications for reservoir location, geometry and facies distribution, and subsurface identification.

Introduction

Mass-transport deposits (MTDs) are the result of gravity-induced mass failures occurring on subaqueous slopes (or, simply, submarine landsliding). They involve the downslope translation of masses of material, often of very large volumes, generally onto regions of lower gradient (e.g. Hampton & Locat, 1996; Owen et al., 2007). They may be extremely mobile (e.g. Mohrig et al., 1998; Gee et al., 1999; Harbitz et al., 2003), and flow over regions with gradients below 1° (Hafliadson et al., 2004). Individual deposits range in volume from a few m^3 to greater than 5,500 km^3, and up to 35,000 km^2 in areal extent (e.g. Jansen et al, 1987; Bugge et al, 1987; Laberg et al, 2002; Lykousis et al, 2002; Maslin and Mikkelsen, 1998; Piper et al, 1997). Mass failures thus include the largest sedimentation events on Earth. They have been identified in both ancient and modern settings, using single channel (high-resolution) and multi-channel seismic, swath bathymetry, core and outcrop data (e.g. Goldfinger et al., 2000; McAdoo et al., 2000; Krastel et al., 2001; Lucente and Pini, 2003; Hozma, 2004), and include deposits described variously as debris flows, slumps and slides (Moscardelli and Wood, 2007). They may comprise a large proportion (locally greater than 50%) of the sediments on the slopes and floors of deep water basins (Posamentier and Walker, 2006).

By redistributing material on the sea-floor, mass failures may significantly re-mould the submarine landscape (Fig. 1). Firstly, removal of material by sliding creates submarine scars that may cover areas of thousands of square kilometers of the sea floor, bounded by relief up to hundreds of meters high in the up-slope region (e.g. Bugge et al., 1987; Goldfinger et al., 2000; Fig. 2). Secondly, depositional topography on and around

the deposit itself may amount to tens of meters (Kneller and Dykstra, 2005; Jackson and Johnson, 2009; Dykstra et al., 2011; Fig. 3) and locally up to 250 meters (Walker, 2008), supported by the yield strength of the materials within the MTD, which can vary greatly within a single deposit. Thirdly, larger events may even move sufficient mass to generate an isostatic response in the lithosphere (McGinnis et al., 1993; Edwards, 2000; Dykstra 2005). Lastly, the emplacement of the deposit itself fills accommodation on the slope and basin-floor. This paper concerns the first two of these.

Depositional systems on submarine slopes and basin floors are dominated by the deposits of sediment gravity flows – principally turbidites and mass transport deposits of various kinds. Since sediment gravity flows inevitably move down the gradient of gravitational potential they are highly sensitive to sea-floor topography. This is especially true of turbidity currents, which may even respond to the subtle topography created by pre-existing individual turbidite beds (e.g. Mutti & Sonino, 1981; Mutti et al., 1999; Al Ja'aidi et al., 2004; Deptuck et al., 2008). The alteration of sea floor topography by mass transport thus affects sediment pathways on the slope, and the distributions of zones of erosion, bypass and deposition from turbidity currents, the latter occurring within relative bathymetric lows or in association with negative gradient changes. Thus the location, nature and geometry of depositional systems dominated by sediment gravity flows, especially turbidite systems, may be profoundly affected by the presence of mass transport deposits or their related slide scars (Brami et al., 2000). In this paper we describe such MTD-associated turbidite systems in terms of the type of space that they occupy, which is governed by its location and the way in which it was generated.

We also draw attention to the possibility that an MTD may remain active after the first event of emplacement, thus creating a dynamic scenario for turbidity current pathways. Such a process of progressive slumping is known in many subaerial environments, and we suggest it is also evident in deep water environments. In such a case, the stratal architecture of the ponded beds is affected by the continued deformation of the MTD, which may include deformation of the MTD surface, growth strata or semi-passive translation on top.

Styles of Accommodation Space

The relative bathymetric lows on and around MTDs constitute accommodation space in the sense that they form available space within which sediment can be deposited (Jervey, 1988). Accommodation space on the slope has been classified in gross stratigraphic and geometric terms by Prather et al. (1998). We define accommodation space for turbidite systems at the local scale (i.e. where dominated by a particular set of depositional processes, such as unconfined turbidity currents) as the space between the existing sediment surface (the sea floor) and the equilibrium depositional surface for the processes in question, for example a fan surface or the floor of a submarine channel (Pirmez et al., 2000; Kneller, 2003; Smith, 2004). The gradient of the equilibrium depositional surface is dictated by factors generally grouped under the term 'flow efficiency' (*sensu* Mutti and Johns, 1978; Mutti, 1979; Mutti et al., 1999; i.e. flow discharge or thickness and proportion of mud, but also flow density; Al Ja'aidi et al., 2004). A similar concept of flow efficiency and graded profiles has been applied also to subaerial fans, where transport efficiency is dictated by the time-averaged discharge flowing to the fan (Milana and Ruzicki, 1999). The gradient of the equilibrium depositional surface varies from

almost horizontal for highly efficient turbidity currents (typically large and/or mud-rich systems), to slopes of several degrees for deposits of highly inefficient flows (typically small and/or sandy systems). This means that accommodation may exist wherever the local slope of the sea-floor is less than the equilibrium depositional slope, even in the absence of three-dimensional topographic enclosure defined by closed bathymetric contours (see, for example, Greene et al., 2006); it also means that the amount of accommodation varies with the type (efficiency) of the turbidite system that is filling it, which may also vary through time due to changes in external factors. In Figure 4 we illustrate the main types of MTD-associated accommodation, which are described in the following sections.

Evacuated Slide Scar

The evacuated scar of a submarine landslide provides a relative bathymetric low that can trap sediment and/or funnel sediment-bearing flows. When located on the upper slope it may capture or redirect down-slope sediment pathways (Kertznus, 2009). The evacuated volume of the slide scar can be up to thousands of km^3 (e.g. Bugge et al., 1988; Garziglia et al., 2008). Slide-scars tend to have a concave-up profile in the dip direction, and a fairly flat floor in the strike direction, commonly related to detachment along a particular stratigraphic horizon, although the detachment commonly steps from one horizon to another. This surface is often overlain by a rubbly residuum of failed and attenuated material, in some cases related to retrogressive failure of the headwall scarp (e.g. Bryn et al., 2003) (Fig. 5). The scar often has a steep headwall and sides, and sometimes a steep down-dip terminus that creates a frontal ramp (e.g. Hampton et al., 1996; Lucente and Pini, 2003).

Many large mass failures occur on the upper slope and cut back into the shelf edge; examples include the East Breaks, Rosetta and Storegga slides (e.g. Piper and Behrens, 2003; Hafliadson et al., 2004; Moscardelli and Wood, 2008; Loncke et al., 2009; Figs 2, 5 and 6). Many of these failures occur within river-fed upper slope sediment accumulations lying directly down-dip of shelf-edge deltas, and form in response to sedimentary loading of the upper slope by these shelf-edge systems. The slide scars may then form a focus for the shelf-edge and upper slope depositional system (as has occurred within the upper part of the East Breaks Slide, see below; Fig. 5), producing packages of clinoforms (including turbidites) that in seismic section can be seen to down-lap the floor of the slide scar (Fig. 7). Turbidite deposition may also be enhanced by flow deceleration associated with the slope break at the base of the headwall scarp.

An ancient example at outcrop may be represented by the Eocene La Jolla Group of Southern California, where an upper slope system has prograded over a surface, cut into older shallow marine and non-marine sediments, that is almost horizontal over seven kilometers of strike extent, representing a putative slide scar (Fig. 8). Upper slope siltstones apparently form downlapping clinoforms onto this surface, capped by a progradational shallow marine succession (May et al., 1983).

Slide scars may also capture the downslope drainage in the form of turbidite channels (Winker and Booth, 2000; Loncke et al., 2009; Kertznus, 2009). The channel system may be entirely contained within the slide scar, as in the case of the late Pleistocene East Breaks Slide, exposed at the sea floor in the western Gulf of Mexico; the slide scar is some 30 km wide at the head-wall where it cuts the shelf break, and extends more than 50 km down-slope (Fig. 5). The scar has captured the principal down-slope

sediment transport pathways in the form of several channel systems, one of which traverses the entire length of the scar to feed the Colorado Fan (Winker & Booth, 2000). Similarly, the late Pleistocene Rosetta Slide, downdip of the modern Nile Delta, cuts the shelf break and has captured the recent downslope sediment transport from the Rosetta branch of the Nile via turbidite channels (Loncke et al., 2009; Kertznus, 2009) (Fig. 6).

The Cretaceous Venado Sandstone (Great Valley sequence, northern California) provides an ancient example of such channel capture within a probable slide scar; this 200 meter thick channel complex rests within a 3 km wide erosional feature with a stratigraphically concordant, flat base against the surrounding Fiske Creek Shale; debris flow deposits form a veneer immediately above this basal surface (Fig. 9), (Lowe, 2004).

Similarly, within the Eocene Hecho Group of northern Spain, erosional features on the slope containing coarse-grained channel or canyon facies (Mutti et al., 1989; Millington and Clarke, 1995) are interpreted as slide scars that have captured the turbidite drainage down the slope (Fig. 10).

The up-dip steep slope of the slide scar also produces an important alteration of the equilibrium profile. As a result erosion is favored in the upper reach of the slide scar, commonly causing gullying, and creating many small-scale transport systems that cause the initial filling of the slide scar by very local sedimentation, as described in seismic sections by Richardson and others (2011).

The late Pleistocene Einstein channel system in the shallow subsurface of the eastern Gulf of Mexico illustrates channel capture in a smaller scale slide scar further down the slope (Hackbarth & Shew, 1994). The c. 100 meter deep, 2 km wide scar (Fig. 11) lies down-dip of a swarm of shelf-edge to upper slope gullies that formed during the

early part of a sea-level lowstand (Posamentier, 2003; Faulkenberry, 2004). The gulley most directly up-dip of the slide scar amplified into a slope channel that captured the turbidity currents to become the principal sediment pathway down this part of the slope; the channel subsequently aggraded out of the slide scar confinement, but its position on the slope was nonetheless determined by the location of the slide scar (Faulkenberry, 2004).

Updip Ponding

The lower end of a slide scar may be partially filled by mass transport deposits derived from the slope failure, or from later retrogressive failures of the slide scar (see for example Amazon Fan mass transport complexes, Piper *et al*., 1997; Sahara Slide, Simm *et al*., 1991). This may result in a local bathymetric low, with or without three-dimensional closure, at the trailing edge of the mass transport deposit, which can act as a pond for subsequent sediment gravity flow deposits (Fig. 12). Complete three-dimensional closure is not a necessary condition for updip ponding, however, since small inefficient turbidite systems may have significant depositional dip (see, for example, Badalini et al., 2000, Posamentier et al., 2000; Al Ja'aidi et al., 2004). For ponding to occur, the mass transport deposit need only divert the sediment transport pathway along routes where the sea-floor gradient is less than the depositional dip on an equilibrium profile (Pirmez et al, 2000; Kneller, 2003; compare Milana and Ruzicki, 1999). These updip lows can range up to a few kilometers wide perpendicular to the slope, tens of meters deep, and can be up to many tens of kilometers long, depending on the size of the MTD itself.

The ponded sections may show either onlap or downlap, depending upon orientation. In some cases small-scale depositional sequences (truncation-onlap) can be observed, suggesting that these accommodation ponds could take long time to fill, while the MTD is still moving by creep (see below; Fig. 13). Greene *et al*., (2006) illustrate Holocene examples of up-dip ponding from offshore California with thicknesses of a few tens of meters, dip extents of a few hundreds of meters to a few kilometers, and strike extents of a few kilometers (Fig. 14a). Large-scale updip ponding has been identified in outcrop (Lucente and Pini, 2003; Dykstra, 2005), and in seismic data (Fig. 14b);

Surface ponding

Mass transport deposits may develop considerable relief on their upper surfaces (e.g. Badalini et al., 2000). This is a consequence of the existence of a yield strength that allows the deposit to maintain a significant surface slope or rugosity (Fig. 3) commonly due to the presence of included blocks of stronger material (McGilvery and Cook, 2003; Hoffman et al., 2004) or due to pressure ridges combined with transverse troughs (e.g. Lee et al., 2004; Fig. 15). Surface relief can result from original depositional topography (either from catastrophic emplacement or creep) or from differential compaction, or a combination of these. In both cases, depositional topography commonly appears to bear some relationship to structures within the mass transport deposit, such as imbrication and folding of slide sheets, normal faults, zones of cleavage, or the presence of blocks (Figs 15, 16). The topography may be relatively smooth or can also occur as a consequence of discrete discontinuities breaking the surface of the deposit, such as extensional faults (producing graben or half-graben, Fig. 17). Surface relief is often oriented approximately perpendicular to the transport direction (for example generating slope-parallel pressure

ridges and furrows which can trap and funnel sediment) but may also mimic the complex orientations of internal structures (Dykstra, 2005; Dykstra et al., 2011).

Extensional faults within MTDs generate accommodation space on the surface of the MTD on at least two different scales. Individual faults create negative relief immediately overlying the subsided hanging wall block (Martinsen et al., 2000; Edwards, 2000; Fig. 17). This creates relatively small amounts of accommodation, on the scale of the fault block, commonly restricted vertically to a few meters or tens of meters, and laterally to a few hundred meters, though in some cases extending for many kilometers (Fig. 17). Fault arrays that produce widespread thinning above a common decollement, on the other hand, can create large subsided zones on the MTD surface over a much larger area, often several km wide and hundreds of meters thick, grading into the rubbly veneer that covers many slide scars (Fig. 5).

Thrust faults are commonly present, especially where the basal surface of the MTD encounters a ramp, the concave-up downdip portion of the slide scar (i.e. where the basal detachment ramps up onto the sea floor; Frey-Martinez et al., 2006; Fig. 18), or other surface roughness underlying the MTD, but may also occur in the absence of basal topography (Figs 19, 20). Thrust faults can occur individually, or in arrays. Surface relief generated by thrusts can be tens of meters high, a few km wide and many km long, and cause partial or full closure of many km^3 of space. As with normal faults, the surface topography commonly reflects the orientation of structures within the MTD, which in the case of thrust systems is commonly curvilinear due to heterogeneous shear, with the topography forming downslope-facing arcs (Fig 15) (e.g. Lee at el., 2004; Dykstra et al., 2011).

However, much or all of the deformation may be entirely plastic in nature rather than occurring along discrete shear planes. Pressure ridges may form as a result of this plastic behaviour in a similar fashion to other irregular and highly viscous plastic flows, such as certain lava flows or rock glaciers. Much of the upper surface may show roughness generated by drag at the base of the flow, in the form of a series of arcuate pressure ridges sub-parallel to the front of the MTD. If the MTD is emplaced as multiple lobes these pressure ridges may be sinuous. The ridges are separated by troughs whose dimension is in general proportional to the size and thickness of the MTD, so the larger the MTD the thicker could be the sediment fill of the trough.

Styles of Supra-MTD Accommodation

The scale, geometry and interconnectivity of the topography play a large part in determining the nature of any turbidite reservoirs that may be formed by ponding on top of the MTD. Spectral analysis of the surface topography on MTDs at the sea-floor shows dominant topographic wavelengths often in the range of a few hundred meters (Fairweather, 2014; Garyfalou, 2014), reflecting the dominant length scales of included blocks and the thickness of imbricated slide sheets. However, both smaller and larger scales of topography may be present, related to smaller and larger wavelength structures such as small blocks and local (non-through-going) thrust structures, and at the larger length-scale, imbricate stacks of normal or thrust-bounded fault blocks (Fig. 19).

The dominant topographic wavelength and amplitude determine the spacing and maximum thickness of isolated ponded or tortuously interconnected sands (sensu Smith, 2004) where the topography is not completely buried by turbidites (under-filled case; Fig. 21). Where the topography is buried by turbidite deposition (overfilled case), the

topographic wavelength determines the form of the base of the reservoir, and perhaps the locations of and the length-scale and depth variation of fluid contacts. These features are scale-dependent since smaller wavelengths of topography may be inundated while larger scales may still create effective confinement.

The nature of the ponded turbidite fill in underfilled cases is likely to be controlled in part by the respective length scales of the topographic relief on the one hand and the thickness and vertical density structure of the turbidity currents on the other (Kneller and McCaffrey, 1999; Kneller and Buckee, 2000; Sequeiros et al., 2010; Meiburg & Kneller, 2010, and references therein). In the case of flows whose thickness is of the same order as the topographic relief, or less, little overspill may occur, resulting in successive filling of the lows down depositional dip in a fill-and-spill style (Fig. 22). Continued infilling leads to the type of tortuously inter-connected bodies described by Smith (2004); ultimately the topography is buried by deposition.

Conversely, where flows are large with respect to the topography, they will over-run it. Nonetheless, sand deposition is likely to be restricted to the topographic lows, since deposition from turbidity currents is highly sensitive to topography and gradient changes (e.g. Kneller & McCaffrey, 1995,). In these situations, much of the flow bypasses from basin to basin, resulting in preferential sand deposition and potentially high net-to-gross in the ponded section (Fig. 22). Where the flows pass over the topographic highs they may erode the typically muddy material of the MTD and produce horizons of shale clasts within the ponded fill. Filling of these topographic lows may be coeval, even though the resulting deposits may not be physically connected; facies relationships are likely to be complex.

Figures 23/24, and Figures 25/26 show examples of underfilled and overfilled topography respectively. In the more sand-poor example of underfilled topography (Fig. 23) there are no indicators of bypass within the sands, which have the appearance of a non-amalgamated confined sheet system, implying that the sand body may be physically disconnected from others overlying the same MTD; however, the common presence of shale clast horizons within the sands may be an indication of erosion over the topographic highs by outsize flows passing from one pond to another. In the more sand-rich example of underfilled topography (Fig. 24) the sands are amalgamated and show evidence of bypass. This sand body appear disconnected in two dimensions from others overlying the same MTD; it may be that outsized flows surmounted and bypassed the topographic highs on the top of the MTD, and the sands are truly isolated, or that they are tortuously connected in three dimensions.

Figure 25 shows a seismic-scale outcrop of middle Carboniferous Paganzo Group sediments from Cerro Bola, NW Argentina (see Dykstra *et al.,* 2011). Figure 26 is a profile of MTD topography generated at the Cerro Bola outcrop. The profile is oriented broadly perpendicular to paleo-flow of the MTD and thus illustrates the span-wise complexity and variation of irregularities produced by MTD topography. These are organised into a scaled hierarchy (cf Armitage *et al.,* 2009) in that many smaller scale basins (short-wavelength and amplitude) are nested within a single larger-scale (long-wavelength and amplitude) depression. Individual beds can be correlated over greater length-scales than the underlying topography, indicating their continuity in three dimensions. The initial topographic irregularities reflect small-scale (10m amplitude, 200-300m wavelength) discrete, isolated basins that evolved over time into intermediate-

scale (c. 500-1000m) partially isolated basins as the smaller scales of topography were filled. The upper units are confined only by the largest topographic wavelength observed (c. 6500m; Figs 25, 26, 27).

Turbidites show changes in the interaction at different topographic scales of infilling, and consequently five units can be identified (Fig. 26 and caption) each with different filling styles. The units vary in occurrence across the topography and the boundaries between them are deformed producing minor unconformities. Flattening along these unit boundaries provides insight into the chronology of generation of the MTD topography, illustrating that the topography neither formed instantaneously nor remained static, but was generated progressively and heterogeneously over time, contemporaneously with turbidite deposition (Fig. 26). As the topography became progressively buried by turbidite deposition, the selective trapping of the coarser sediment load by the topographic lows became less effective.

Further evidence of this syn-depositional evolution of the MTD topography is also suggested by seismic examples (Fig. 12) in which it can be observed that the lower ponded turbidites are more deformed than the upper ones. This suggest that while some MTDs may be emplaced as a discrete or single event, others may be emplaced episodically, and perhaps others could be entirely emplaced by creep.

Not all scales of MTD topography show the fill-and-spill style that is commonly seen in turbidites in topographically confined settings (Prather *et al.,* 2003; Brunt *et al.,* 2004; Sinclair & Tomasso, 2004) but may exhibit a variety of trends related to turbidity current interaction with topography of varying scale and geometry, as well as possible variations in turbidity current character.

Implications for reservoir

The various mechanisms by which MTDs create accommodation are important for the sequestration of sediment on the slope. The potential to fill this accommodation depends upon (a) the sediment supply, and (b) the interval between sealing mass transport events. Whether individual reservoir 'ponds' remain isolated (underfilled) or become interconnected (overfilled) producing more continuous reservoir (whose basal geometry may nonetheless be complex) depends on sediment supply rates compared to MTD recurrence time and the size of the topographic relief. The maximum thickness of isolated ponds (underfilled case), or the amplitude of base-reservoir relief (overfilled case) is limited to the scale of supra-MTD relief – a few tens of meters. By contrast, slide scar fills may be an order of magnitude greater in thickness.

The geometry and areal extent of many reservoirs will directly mimic that of the immediately underlying MTD-related topography, and so will depend on which of the accommodation styles described above is being filled.

Depositional turbidity currents are extremely sensitive to topography (Kneller & McCaffrey, 1995; Al Ja'aidi et al., 2004) since deceleration of turbidity currents, which triggers deposition, is related to divergence of streamlines, which may be induced by flow deflection around topography, or by gradient changes; Kneller and McCaffrey (1995) show that deposition rate - and therefore deposit thickness - is a function of the topographic curvature, i.e. the first derivative of the gradient. Therefore, in settings where mass failures have created local topography on the seafloor, especially where that topography is complex and widespread (e.g. Fig. 1) and leads to flow deflection or

changes of gradient in the flow direction, the depositional effect on currents flowing over the seafloor will be considerable. Exactly how these effects will be expressed in terms of deposition, erosion, and final facies and thickness distribution of sediment from turbidity currents will depend largely on (a) the relationship between the scale of the turbidity currents (thickness, stratification, grain-size distribution), and the scale and geometry of the topography on the seafloor; (b) the orientation of MTD-induced bathymetry with respect to the regional slopes; (c) the pathway taken by the turbidity currents over the surface of the MTD; and (d) the ratio between areas with positive potential accommodation space and those without.

As illustrated above, supra-MTD topography may evolve gradually, even when initial emplacement of the deposit was catastrophic (e.g. Bondevik et al., 2005). This may result in complex internal growth stratigraphy, as illustrated in Figures 12 and 13. In these cases, accommodation space is therefore created or destroyed after emplacement, and thus, the resulting stratigraphy within ponds will depend also on the rate of creation of accommodation space, and the evolution of the areas of accommodation that is positive (i.e. bumps surrounded by continuous valleys), neutral or negative (i.e. ponds surrounded by continuous ridges). As some MTDs may continue their downslope movement it is likely some sediments will be eroded over developing seafloor highs, as occurs in growth structures. In particular, updip ponded turbidites may have more potential for this further transport and progressive tilting (Fig. 12) due to the position near the main detachment (the slide scar). Post-emplacement movements, including compaction, may also be instrumental in trap formation, and in disconnecting originally continuous reservoirs which may nonetheless remain in pressure communication

Conclusions

We have presented some general observations about the role of mass transport deposits in the alteration of accommodation on continental slopes, and their effect on turbidity currents and turbidite reservoir systems. Mass-transport deposits at all scales have an effect on turbidite systems. Large-scale mass-failures may significantly re-mould the seafloor over wide areas, creating conditions that determine a unique distribution of stratigraphic traps on the slope, and the geometry and facies of the reservoirs developed within them. By redistributing large volumes of sediment on the seafloor, mass failures affect turbidity current pathways down the slope, and generate volumetrically significant accommodation within the slide scar, usually accumulating coarser sediments than on the surrounding slope, due to the preferential accumulation of the coarser fractions within local lows. This local accommodation commonly occurs around and on top of the mass transport deposit. The size and geometry of these local lows is generally controlled by the internal structure of the mass-transport deposit itself, but the manner in which they are filled depends on the complex interplay between the topography and the turbidity currents that flow into or over them.

Similar supra-MTD turbidite sand bodies seen in adjacent wells, with biostratigraphically unresolvable age difference and occupying identical stratigraphic positions atop the same MTD, may nonetheless be entirely disconnected from one another if they underfill the local ponded accommodation space. Such discontinuity should always be suspected in sands overlying MTDs, especially where fluid contacts

vary between adjacent wells. Variable fluid contacts may also be present where the local ponded accommodation space is overfilled or tortuously connected.

Acknowledgments

The work summarized in this paper was supported under a succession of joint industry projects between 2002 and 2012 by Anadarko, BG, BP, BHP-Billiton, ConocoPhillips, Chevron, DONG, GDF Suez, Hess, Maersk, Marathon, Murphy, Petrobras, Statoil, Woodside, Hess, Petrobras, Total, StatoilHydro, RWE Dea. We thank BG, BHP Billiton, Shell and Western Geco for use of seismic data, and Vanessa Kertznus, Sacha Tremblay, Laura Faulkenberry and Katerina Garyfalou for use of unpublished data and interpretations.

References

Al ja′aidi , O.S., W.D. McCaffrey, & B.C. Kneller, 2004,The influence of turbidity current flow efficiency upon deposit geometry: implications for sand body architecture in confined basins, *in* S. Lomas & P. Joseph, eds, Confined turbidite systems: Geological Society of London Special Publication 222, p. 45-58

Armitage, D.A., Romans, B.W., Covault, J.A. and Graham, S.A., 2009. The influence of mass-transport-deposit surface topography on the evolution of turbidite architecture: The sierra contreras, tres pasos formation (Cretaceous), Southern Chile. *Journal of Sedimentary Research,* **79**(5-6), pp. 287-301.

Badalini, G., B.C. Kneller, and C.D. Winker, 2000, Architecture and processes in the Late Pleistocene Brazos-Trinity turbidite system, Gulf of Mexico continental slope: *in* P. Weimer, R.M. Slatt, J. Coleman, J., N.C. Rosen, H. Nelson, A.H. Bouma, M.J. Styzen, and D.T. Lawrence, eds, Deep-water reservoirs of the world: Gulf Coast Section, SEPM 20th Annual Research Conference, CD-ROM, p. 16–33.

Bondevik, S., Løvholt, F., Harbitz, C., Mangerud, J, Dawson, A. & Svendsen, J.I., 2005. The Storegga Slide tsunami—comparing field observations with numerical simulations. Marine and Petroleum Geology, **22**, 195–208.

Brami, T.R. C. Pirmez, A. Curtis, S. Heeralal, and K.L. Holman, 2000, Late Pleistocene deep-water stratigraphy and depositional processes, offshore Trinidad and Tobago, *in* P. Weimer, R.M. Slatt, J. Coleman, J., N.C. Rosen, H. Nelson, A.H. Bouma, M.J. Styzen, and D.T. Lawrence, eds, Deep-water reservoirs of the world: Gulf Coast Section, SEPM 20th Annual Research Conference, CD-ROM, 104-115.

Brunt, R.L., Mccaffrey, W.D. and Kneller, B.C., 2004. Experimental modeling of the spatial distribution of grain size developed in a fill-and-spill mini-basin setting. *Journal of Sedimentary Research,* **74**(3), pp. 438-446.

Bryn, P., A. Solheim, K. Berg, R. Lien, C.F. Forsberg, H. Haflidason, D. Ottesen, and L. Rise, 2003, The Storegga Slide complex; Repeated large scale sliding in response to climatic cyclicity, *in* J. Locat and J. Mienert, eds, Submarine mass movements and their consequences: Kluwer Academic Press, The Netherlands, p. 215–222.

Bugge, T., S. Befring, R.H. Belderson, T. Eidvin, E. Jansen, N.H. Kenyon, H. Holtedahl, H., and H.P. Sejrup, 1987, A giant three-stage submarine slide off Norway: Geo-Marine Letters, v. 7, p. 191-198.

Bugge, T., R.H. Belderson, and N.H. Kenyon, 1988, The Storegga Slide: Philosophical Transactions of the Royal Society of London, Series A, Mathematical and Physical Sciences, v. 325, p. 357-388.

Deptuck, M.E., Piper, D.J.W., Savoye, B._ and Gervais, A., 2008. Dimensions and architecture of late Pleistocene submarine lobes off the northern margin of East Corsica. Sedimentology**, 55**, 869–898

Dykstra, M., 2005, Dynamics of sediment mass-transport from the shelf to the deep sea Unpubl. Ph.D. thesis, Santa Barbara, University of California, 152 p.

Dykstra, M., B. Kneller, and J.P. Milana, 2006, Deglacial and postglacial sedimentary architecture in a deeply incised paleovalley-paleofjord—The Pennsylvanian (late Carboniferous) Jejenes Formation, San Juan, Argentina: Geological Society of America Bulletin, v. 118, p. 913-937.

Dykstra, M., Garyfalou, K., Kertznus, V., **Kneller, B.C.**, Milana, J.P., Molinaro, M., Szuman, M & Thompson, P., 2011. Mass-transport deposits: combining outcrop studies and seismic forward modeling to understand lithofacies distributions, deformation, and their seismic expression. In Posamentier, H., Weimer P. & Shipp, C. *SEPM Special Publication 95*, 293-310.

Edwards, M. B., 2000, Origin and significance of retrograde failed shelf margins; Tertiary Northern Gulf Coast Basin. Gulf Coast Association of Geological Societies Transactions, v. L, p. 81-93.

Frey-Martínez, J., Cartwright, J and James, D., 2006. Frontally confined versus frontally emergent submarine landslides: A 3D seismic characterization. Marine and Petroleum Geology, **23**, 585–604.

Fairweather, L., 2014. Mechanisms of supra MTD topography generation and the interaction of turbidity currents with such deposits. Unpublished PhD Thesis, Geosciences, University of Aberdeen, 242pp.

Faulkenberry, L., 2§§004, High-resolution seismic architecture of upper slope submarine channel systems: Gulf of Mexico and offshore Nigeria: Unpublished PhD Thesis, Earth Sciences, University of Leeds, 258pp.

Garyfalou, K. 2014. Integrated analysis of mass- transport deposits: Outcrop, 3D seismic interpretation and fast fourier transform. Unpublishe PhD thesis, University of Aberdeen.

Garziglia, S., S. Migeon, E. Ducassou, L. Loncke, and J. Mascle, 2008, Mass-transport deposits on the Rosetta province (NW Nile deep-sea turbidite system, Egyptian margin): Characteristics, distribution, and potential causal processes: Marine Geology, v. 250, p. 180–198.

Gee, M.J.R., D.G. Masson, A.B. Watts, and P.A. Allen, 1999, The Saharan debris flow: an insight into the mechanics of long runout submarine debris flows: Sedimentology, v. 46, p. 317-335.

Goldfinger, C. K., D. LaVerne, L.C. McNeill, and P. Watts, 2000, Super-scale failure of the southern Oregon Cascadia margin: Pure and Applied Geophysics, v. 157, no. 6-8, p. 1189-1226.

Greene, H.G., L.Y. Murai, P. Watts, N.A. Maher, M.A. Fisher, C.E. Paull, and P. Eichhubl, 2006, Submarine landslides in the Santa Barbara Channel as potential tsunami sources: Natural Hazards and Earth System Sciences, v. 6, p. 63–88

Hackbarth, C.J., and R.D. Shew, 1994, Morphology and stratigraphy of a mid-Pleistocene turbidite leveed channel from seismic, core and log data, northeastern Gulf of Mexico, *in* P. Weimer, A.H. Bouma, and B.F. Perkins, eds., Submarine fans and turbidite systems: Gulf Coast Section, SEPM, 15th Annual Research Conference, p. 127-133.

Haflidason, H., H.P. Sejrup, A. Nygard, J. Mienert, P. Bryn, R. Lien, C.F. Forsberg, K. Berg, and D. Masson, 2004, The Storegga Slide: architecture, geometry and slide development: Marine Geology, v. 213, p. 201-234.

Hampton, M.A., H.J. Lee, and J. Locat, 1996, Submarine landslides: Reviews of Geophysics, v. 34, p. 33-59.

Harbitz, C., G. Parker, A. Elverhoi, J. Marr, D. Mohrig, and P. Harff, P., 2003, Hydroplaning of subaqueous debris flows and glide blocks: Analytical solutions and discussion: Journal of Geophysical Research-Solid Earth, v. 108, p. 2349–2366

Homza, T. X., 2004, A structural interpretation of the Fish Creek Slide (Lower Cretaceous), northern Alaska: AAPG Bulletin, v. 88, p. 265-278.

Jackson, C.A-L. and H. Johnson, 2009, Sustained turbidity currents and their interaction with debrite-related topography; Labuan Island, offshore NW Borneo, Malaysia: Sedimentary Geology, v. 219, p. 77-96

Jervey, M.T., 1988, Quantitative geological modelling of siliciclastic rock sequences and their seismic expression: *in* C.K. Wilgus et al., Sea-level changes: An integrated approach (Eds), SEPM Special Publication 42, p. 47-69.

Kertznus, V. and Kneller, B.C., in press, Impact of mass-transport processes on deep-water sedimentation and sequence stratigraphic principles: Geology.

Kneller, B.C., 2003, The influence of flow parameters on turbidite slope channel architecture: Marine & Petroleum Geology, v. 20, p. 901-910.

Kneller, B.C. and C.M. Buckee, 2000, The structure and fluid mechanics of turbidity currents; a review of some recent studies and their geological implication: Sedimentology, v. 47, (Supplement 1), p. 62-94.

Kneller, B and M. Dykstra, 2005, Mass transport deposits and slope accommodation (abs): AAPG Annual Meeting Calgary Expanded Abstracts.

Kneller, B., M. Dykstra, P. Thompson, V. Kertznus, M. Szuman, K. Garyfalou, M. Molinaro, M. Huuse, P. Butterworth, D. Macdonald, and J.P. Milana, 2006, Mass transport deposits: combined outcrop studies, 3d seismic interpretation and forward modelling (abs) AAPG Annual Meeting Expanded Abstracts .

Kneller, B.C. and W.D. McCaffrey, 1995, Modelling the effects of salt-induced topography on deposition from turbidity currents: *in* C.J. Travis, H. Harrison, M.R. Hudeac, B.C. Vendeville, F.J. Peel, and R.F. Perkins, eds, Salt, sediment and hydrocarbons. SEPM, 16th Annual Research Conference, p. 137-145.

Kneller, B.C. and W.D. McCaffrey, 1999, Depositional effects of flow non-uniformity and stratification within turbidity currents approaching a bounding slope: deflection, reflection and facies variation: Journal of Sedimentary Research, v. 69, p. 980-991.

Krastel, S., H.U. Schmincke, C.L. Jacobs, R. Rihm, T.P. Le Bas, and B. Alibes, 2001, Submarine landslides around the Canary Islands. Journal of Geophysical Research B: Solid Earth, v. 106: p. 3977-3997.

Lee, C., Nott, J.A., Keller, F.B. & Parrish, A.R., 2004. Seismic expression of Cenozoic mass transport complexes, deepwater Tarfaya-Agadir basin, offshore Morocco. Offshore Technology Conference 16741

Lucente, C.C. and G.A. Pini, 2003, Anatomy and emplacement mechanism of a large submarine slide within a Miocene foredeep in the northern Apennines, Italy: a field perspective: American Journal of Science, v. 303, p. 565-602.

Loncke, L., V. Gaullier, L. Droz, E. Ducassou, S. Migeon, and J. Mascle, 2009, Multi-scale slope instabilities along the Nile deep-sea fan, Egyptian margin: A general overview. Marine and Petroleum Geology, v. 26, p. 633–646.

Lowe, D.R., 2004, Deep-water Sandstones: Marine canyon to basin plain, Western California. AAPG Special Publication, Tulsa, Oklahoma, U.S.A. and The Pacific Section AAPG Bakersfield, California, U.S.A.

Martinsen. O.J., T. Lien, and R.G. Walker, 2000, Upper Carboniferous deep water sediments, Western Ireland; analogues for passive margin turbidite plays: *in* P. Weimer, R.M. Slatt, J. Coleman, J., N.C. Rosen, H. Nelson, A.H. Bouma, M.J. Styzen, and D.T. Lawrence, eds, Deep-water reservoirs of the world: Gulf Coast Section, SEPM 20th Annual Research Conference, CD-ROM, p. 533-555.

May, J.A., J.E. Warme, and R.A. Slater, 1983, Role of submarine canyons on shelfbreak erosion and sedimentation: modern and ancient examples: *in* D.J. Stanley and G.T. Moore, eds., The Shelfbreak: Critical Interface on Continental Margins: SEPM, Special Publication, No. 33, p. 3 15-332.

May, J. A., Lohmar, J.M., Warme, J.E. and Morgan, S., 1991, Field trip guide: Early to Middle Eocene La Jolla Group of Black's Beach, La Jolla, California, in: Eocene Geologic History San Diego Region, Pacific Section. Eds., P. L. Abbott and J. A. May, Pacific Section SEPM, 68: 27-36.

May, J.A., and J.E. Warme, 2000, Bounding surfaces, lithologic variability, and sandstone connectivity within submarine-canyon outcrops, Eocene of San Diego, California. : *in* P. Weimer, R.M. Slatt, J. Coleman, J., N.C. Rosen, H. Nelson, A.H. Bouma, M.J. Styzen, and D.T. Lawrence, eds, Deep-water reservoirs of the world: Gulf Coast Section, SEPM 20th Annual Research Conference, CD-ROM, p. 556-577.

McAdoo, B. G., L.F. Pratson, and D.L. Orange, 2000, Submarine landslide geomorphology, US continental slope: Marine Geology, v. 169, p. 103-136.

McGilvery, T.A. and D.L. Cook, 2003, The influence of local gradients on accommodation space and linked depositional elements across a stepped slope profile, offshore Brunei: *in* H.H. Roberts, N.C. Rosen, R.H. Fillon and J.B. Anderson, eds, Shelf margin deltas and linked down slope petroleum systems: Global significance and future exploration potential: Gulf Coast Section, SEPM 23rd Annual Research Conference, CD-ROM, p. 387–419.

McGinnis, J.P., N.W. Driscoll, G.D. Karner, W.D. Brumbaugh and N. Cameron, 1993, Flexural response of passive margins to deep-sea erosion and slope retreat: implications for relative sea-level change: Geology, v.21, p. 893-896

Meiburg M.E. & Kneller, B.C., 2010. Turbidity currents and their deposits. Annual Reviews of Fluid Mechanics, 42, 135-56.

Millington, J.J. and J.D. Clark, 1995, The Charo/Arro canyon-mouth sheet system, south-central Pyrenees, Spain; a structurally influenced zone of sediment dispersal: Journal of Sedimentary Research, v. 65, p. 443-454.

Moscardelli, L., L. Wood, and P. Mann, 2006, Mass-transport complexes and associated processes in the offshore area of Trinidad and Venezuela: AAPG Bulletin, v. 90, p. 1059-1088.

Moscardelli, L. and L. Wood, 2007, New classification system for mass transport complexes in offshore Trinidad: Basin Research, v. 20, p. 73-98.

Mutti, E., 1979, Turbidites et cones sous-marins profonds: *in* P. Homewood, ed, Sedimentation detritique (fluvial, littoral et marine): Institut de Geologie, Universite de Fribourg, Suisse, p. 353-419.

Mutti, E. and D.R. Johns, 1978, The role of sedimentary bypassing in the genesis of fan-fringe and basin plain turbidites in the Hecho Group system (south-central Pyrenees). Memorie della Società Geologica Italiana 18, p. 15-22.

Mutti, E., M. Seguret, and M. Sgavetti, 1989, Sedimentation and deformation in the Tertiary Sequences of the Southern Pyrenees: American Association of Petroleum Geologists Mediterranean Basins Conference, Guidebook Field Trip No.7, Nice: Special Publication of the Institute of Geology, University of Parma, 157 p.

Mutti, E., R. Tinterri, E. Remacha, N. Mavilla, S. Angella, and L. Fava, 1999, An introduction to the analysis of ancient turbidite basins from an outcrop perspective. AAPG Course Notes 39, 93 pp.

Owen, M., S. Day, and M. Maslin, 2007, Late Pleistocene submarine mass movements: occurrence and causes: Quaternary Science Reviews, v. 26, p 958–978

Piper, J.N. and E.W. Behrens, 2003, Downslope sediment transport processes and sediment distributions at the East Breaks, northwest Gulf of Mexico: *in* H.H. Roberts, N.C. Rosen, R.H. Fillon and J.B. Anderson, eds, Shelf margin deltas and linked down slope petroleum systems: Global significance and future exploration potential: Gulf Coast Section, SEPM 23rd Annual Research Conference, CD-ROM, p. 359–385.

Parsons, J.D., W.J. Schweller, C.W. Stelting, J.B. Southard, W.J. Lyons, and J.P. Grotzinger, 2002, A preliminary experimental study of turbidite fan deposits: Journal of Sedimentary Research, v. 72, p. 619-628.

Pirmez, C., R. T. Beauboeuf, S.J. Friedman, and D.C. Mohrig, 2000, Equilibrium profile and baselevel in submarine channels: examples from late Pleistocene systems and implications for the architecture of deepwater reservoirs: *in* P. Weimer, R.M. Slatt, J. Coleman, J., N.C. Rosen, H. Nelson, A.H. Bouma, M.J. Styzen, and D.T. Lawrence, eds, Deep-water reservoirs of the world: Gulf Coast Section, SEPM 20th Annual Research Conference, CD-ROM, p. 782-805.

Posamentier, H., 2003, A linked shelf-edge delta and turbidite slope-channel turbidite system: 3D seismic case study from the eastern Gulf of Mexico: *in* H.H. Roberts, N.C. Rosen, R.H. Fillon and J.B. Anderson, eds, Shelf margin deltas and linked down slope petroleum systems: Global significance and future exploration potential: Gulf Coast Section, SEPM 23rd Annual Research Conference, CD-ROM, p. 115-134.

Posamentier, H.W. and Walker, R.G., 2006, Deep-water turbidites and submarine fans: *in* H.W. Posamentier and R.G. Walker, eds, Facies Models Revisited SEPM Special Publication 84, p. 399-520.

Prather, B.E., 2003. Controls on reservoir distribution, architecture and stratigraphic trapping in slope settings. *Marine and Petroleum Geology,* **20**(6-8), pp. 529-545

Prather, B.E., J.R. Booth, G.S. Steffens, P.A. Craig, 1998, Classification, lithologic calibration, and stratigraphic succession of seismic facies of intraslope basins, deep-water gulf of Mexico: AAPG Bulletin, v. 82, p. 701-728.

Richardson, S. E. J., Davies, R. J., Allen, M. B. and Grant, S. F. (2011), Structure and evolution of mass transport deposits in the South Caspian Basin, Azerbaijan. *Basin Research*, 23: 702–719. doi: 10.1111/j.1365-2117.2011.00508.x.

Sequeiros, O.E., Spinewine, B., Beaubouef, R.T., Sun, T., García, M.H & Parker, G., 2010. Characteristics of velocity and excess density profiles of saline underflows and turbidity currents flowing over a mobile bed. Journal of Hydraulic Engineering. V. 136, 412-443.

Sinclair, H.D. and Tomasso, M., 2002. Depositional evolution of confined turbidite basins. *Journal of Sedimentary Research,* **72**(4), pp. 451-456.

Smith, R.D.A., 2004, Silled sub-basins to connected tortuous corridors; sediment distribution systems on topographically complex sub-aqueous slopes: *in* S. Lomas, and P. Joseph, Geological Society of London Special Publication 222**,** 23-43

Walker, Donald. Topographic Controls on Deep-Water Sedimentation Patterns–The Casaglia Monte Della Colonna Submarine Slide, Marnoso-Arenacea Formation (Miocene), Northern Italian Apennines. 2008, Ms Thesis, Colorado School of Mines, Golden, Colorado. 184 pp.

Winker, C.D, & Booth, J.R., 2000, Sedimentary dynamics of the salt-dominated continental slope, Gulf of Mexico: integration of observations from the seafloor, near surface and deep subsurface. *in* P. Weimer, R.M. Slatt, J. Coleman, J., N.C. Rosen, H. Nelson, A.H. Bouma, M.J. Styzen, and D.T. Lawrence, eds, Deep-water reservoirs of the world: Gulf Coast Section, SEPM 20th Annual Research Conference, CD-ROM, p. 1059-1086.

Figures

Figure 1

Example of the creation of diverse types of topography on the modern sea floor by mass transport, offshore Brunei. The image covers an area of approximately 10,000 km^2. Seismic data courtesy of BHP Billiton.

Figure 2

The Holocene Storegga slide, offshore Norway, showing the area of negative relief in the evacuated slide scar (ESS) and the extent of the mass transport deposit that has been extruded over the contemporaneous sea floor (from Dykstra, 2005; bathymetry based on ETopo2).

Figure 3

(a) High-resolution 2D seismic section showing 40 m of surface relief on an MTD within a minibasin. The overlying fan laps onto the upper surface of the MTD. Basin IV, Trinity-Brazos system (Late Pleistocene), upper slope, US Gulf of Mexico.

(b) Isochore map of the MTD

(c) Isochore map of the overlying fan, illustrating how the form of the fan is partially determined by this onlap. (Seismic mapping courtesy of G. Badalini. Seismic data courtesy of Shell)

Figure 4

Cartoon illustrating styles of accommodation associated with MTDs

Figure 5

Rendered bathymetry of the sea floor, East Breaks, US Gulf of Mexico, showing slide scar cutting the shelf break, with a rubbly residuum of failed material on the slide scar, subsequent progradation of shelf edge into the head of the slide scar, and partial filling of the scar with turbidite channel systems. Width of view c. 35 km. Data from NOAA.

Figure 6

Rosetta Slide area, Nile Cone, Egypt; variance map 40 ms below sea bed, showing the area of the late Pleistocene Rosetta slide cutting the shelf break, filled by younger mass transport deposits and turbidite channels, culminating in the Rosetta Canyon. Seismic data courtesy of BP. (Modified from Kertznus, 2009. See also Loncke et al., 2009)

Figure 7

Upper slope, offshore Egypt, showing downlap of clinoforms onto the floor of a slide scar that cuts the shelf break. Seismic mapping by S. Tremblay. Data courtesy of BG. (See also Fig. 8)

Figure 8

Cartoon of the stratigraphy of the La Jolla Group (Eocene) exposed in cliffs at Black's Beach, La Jolla, California (modified from May et al., 1983, and May et al., 1991); upper slope clinoforms downlapping a putative slide scar cut into older shelfal sediments.

Shallow marine shelf sediments prograde over channelized slope sediments (See also May and Warme, 2000)

Figure 9

Capture of channel systems within a putative slide scar; Venado Sandstone, Great Valley Sequence (Cretaceous), Berryessa Dam, northern California (Figure redrawn from Lowe, 2004)

Figure 10.

Cartoon based on Hecho Group, Ainsa area, southern Pyrenees, showing the slope, MTD-dominated muddy slope apron at the base of slope, and basin floor. Slide scars on the slope act to capture downslope transport

Figure 11

A) Einstein Channel, eastern Gulf of Mexico, modified from Faulkenberry (2004). Seismic data courtesy of Shell. B) An interpreted slide-scar with gullying from Cerro Bola outcrop (Carboniferous W-Argentina) with indication of the scale of incised channels. C) A detailed view of one incised valley and the slide scar surface

Figure 12

An MTD and interpreted stratigraphy of updip ponded deposits. The truncation-onlap sequences observed and sediment tilting suggest that the MTD was moving downslope

slowly after emplacement. Coloring suggests several stages of successive MTDs amalgamated. Scale division is 100 ms TWTT .

Figure 13

A. Fanning turbidite stratigraphy represents growth strata atop an MTD, inferring creep following initial-emplacement and during turbidite sedimentation. B. line drawing; detail photo shows upper contact of MTD (boxed area); human in upper left for scale.

Figure 14

A. Ponding of turbidites up-dip of MTDs, offshore Santa Barbara, California. Note seaward-dipping sea floor beneath (from Greene et al., 2004). B. Ponding of turbidites up-dip of and atop MTD. Interpreted (above) and uninterpreted (below) seismic sections exhibiting ponding updip of a compressional zone in the MTD, as well as thrust-top ponding (in mini piggyback basins). The dashed lines follow discontinuities within the MTD. Pleistocene, US Gulf of Mexico. Seismic data courtesy of BHP Billiton and Western Geco. (Modified from Dykstra, 2005).

Figure 15

A. Schematic illustrating the relationship between internal/basal structure and superficial accommodation. B. time-slice showing downslope convexity of imbricate slices within MTD; width of field c. 3km. C. 3D cube showing downslope-convex imbricates with back-thrust geometry (up-slope vergence). Seismic data B & C courtesy of BG Group; interpretation by K. Garyfalou (modified from Garyfalou, 2014)

Fig 16

Infilling by turbidites of supra-MTD relief generated by internal structures within the MTD; Miocene Casaglia Monte della Colonna slide, northern Apennines, Italy.

Figure 17

3D visualization of a faulted reflector within a mass transport deposit, illustrating multidirectional extensional faults. Pleistocene, Gulf of Mexico. Data courtesy of BHP Billiton.

Figure 18

Schematic illustration of imbricates associated with a footwall ramp; modified from Lucente and Pini, 2003.

Figure 19

Seismic section showing the generation of long wavelength topographic relief by the formation of imbricate stacks within an MTD. Seismic data courtesy of BG Group.

Figure 20

Imbricates within an MTD apparently unrelated to basal topography, immediately above smooth basal detachment surface. Paganzo Group (Carboniferous), Cañon de la Peña, San Juan Province, Argentina. Humans in lower right for scale.

Figure 21

Cartoon illustrating the effect of under-filled versus over-filled accommodation on reservoir. A. Under-filling of topography by sandy turbidites produces isolated sand bodies whose horizontal dimensions are related to the dominant wavelengths of topography on top of the MTD. These sand bodies are of near-identical age, overlying the same MTD and are typically overlain by hemipelagic sediments of equivalent age. Their degree of connectivity is determined by the distribution of sill heights between adjacent topographic lows; where these are generally low (positive topography – bumps separated by continuous troughs) the sand bodies may be connected in three dimensions, even though discontinuous; where the sills are high (negative topography – ponds separated by continuous ridges) the sand bodies will be disconnected until the intervening ridges are buried. B. Over-filling of topography produces continuous sand bodies with irregular bases, in which laterally variable fluid contacts may be determined by the distribution sill heights. Since topography may exist at several scales, progressive filling will produce ponded fills of increasing scale.

Figure 22

Cartoon illustrating the effect of flow size relative to topographic relief.

Figure 23

Surface ponding, underfilled moderate net-to-gross; Hecho Group (Eocene), Ainsa, northern Spain. A. overview of part of lenticular sand body between MTDs. B. Detail of sheet-like character of ponded sands. C. Detail of local sand onlap onto MTD.

Figure 24

Surface ponding, underfilled; high net-to-gross; Paganzo Group (Carboniferous), Cañon de la Peña, San Juan Province, Argentina.

Figure 25

Large wavelength ponding on top of MTD, Paganzo Group (late Carboniferous), Cerro Bola, La Rioja Province, NW Argentina.

Figure 26. Span-wise profile of MTD topography and supra-MTD turbidite infill developed from outcrop data from Paganzo Group (late Carboniferous), Cerro Bola, Argentina. Illustrates the complexity and variation scales of surface topography. Unit A: a single turbidite that drapes that MTD topography; lateral thickness variations on the meters scale reflect the variation and healing of small-scale topography. Unit B: A stratigraphically continuous varve unit with drop-stones. Unit A and B are overlain by units C, D and E which are turbidite units. Unit C: massive thick-bedded (1-3m) sandstones with equally thick mud-caps. Unit D: finer-grained massive to rippled beds that taper laterally defining lobes. Unit E: thick-bedded (2-4m), course, sands that are commonly inversely graded and channelized

Figure 27. Locality as above; view of the onlap terminations of these ponded turbidites against MTD surface topography.

Figure 1

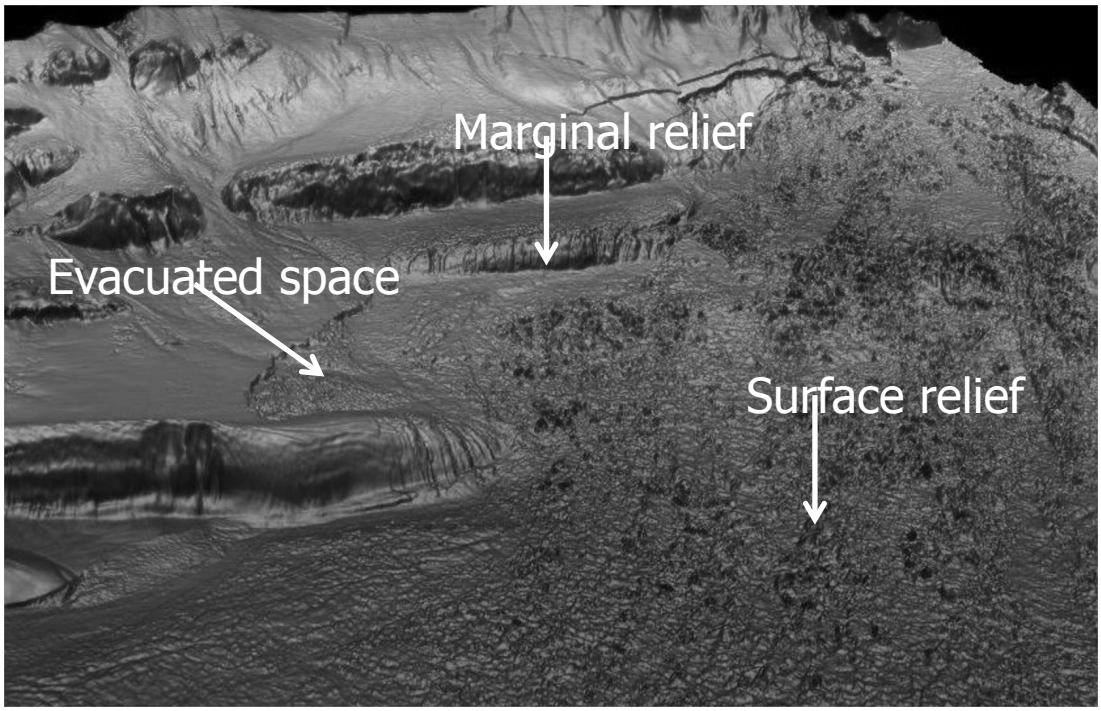

Figure 2

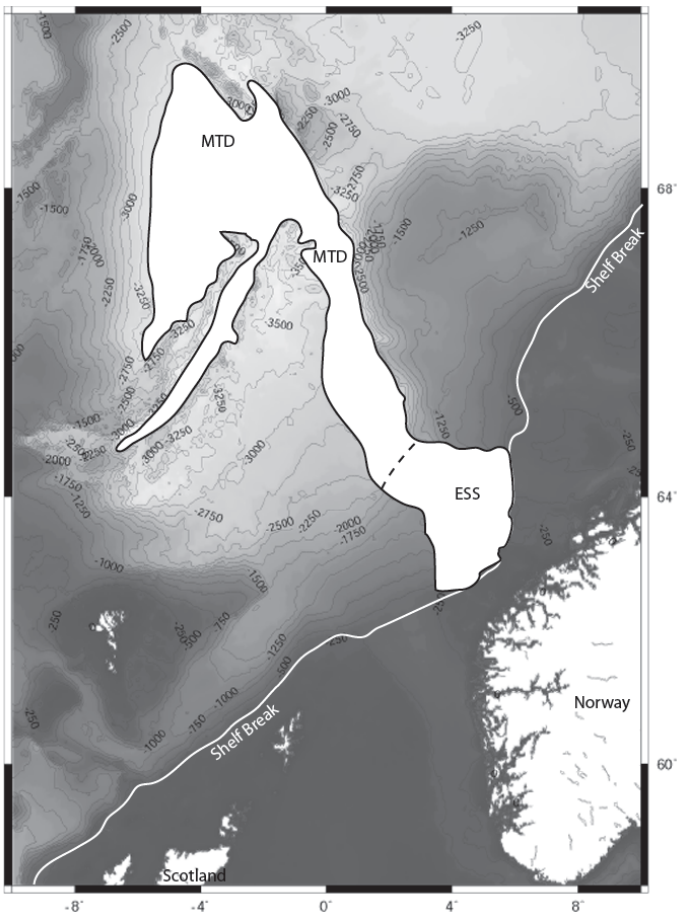

Figure 3

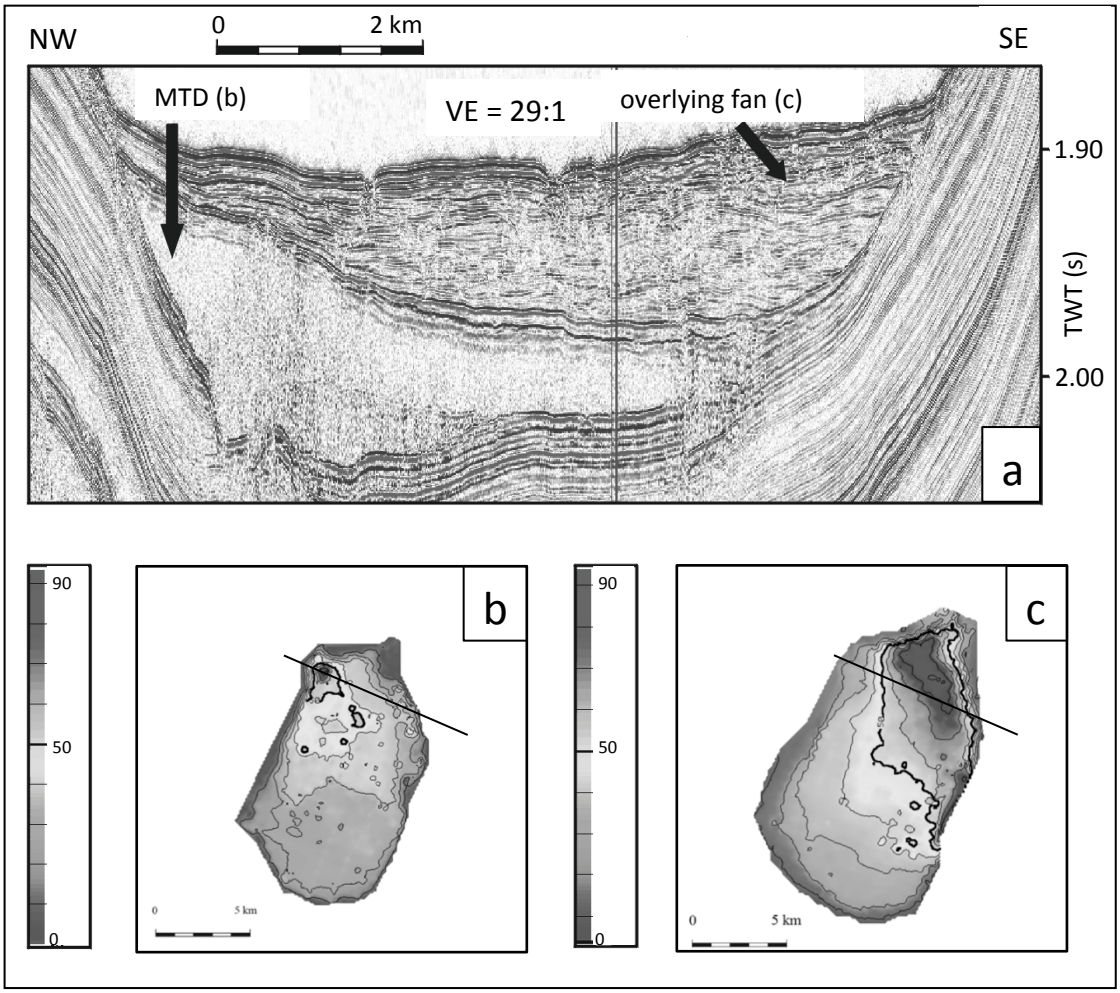

Figure 4

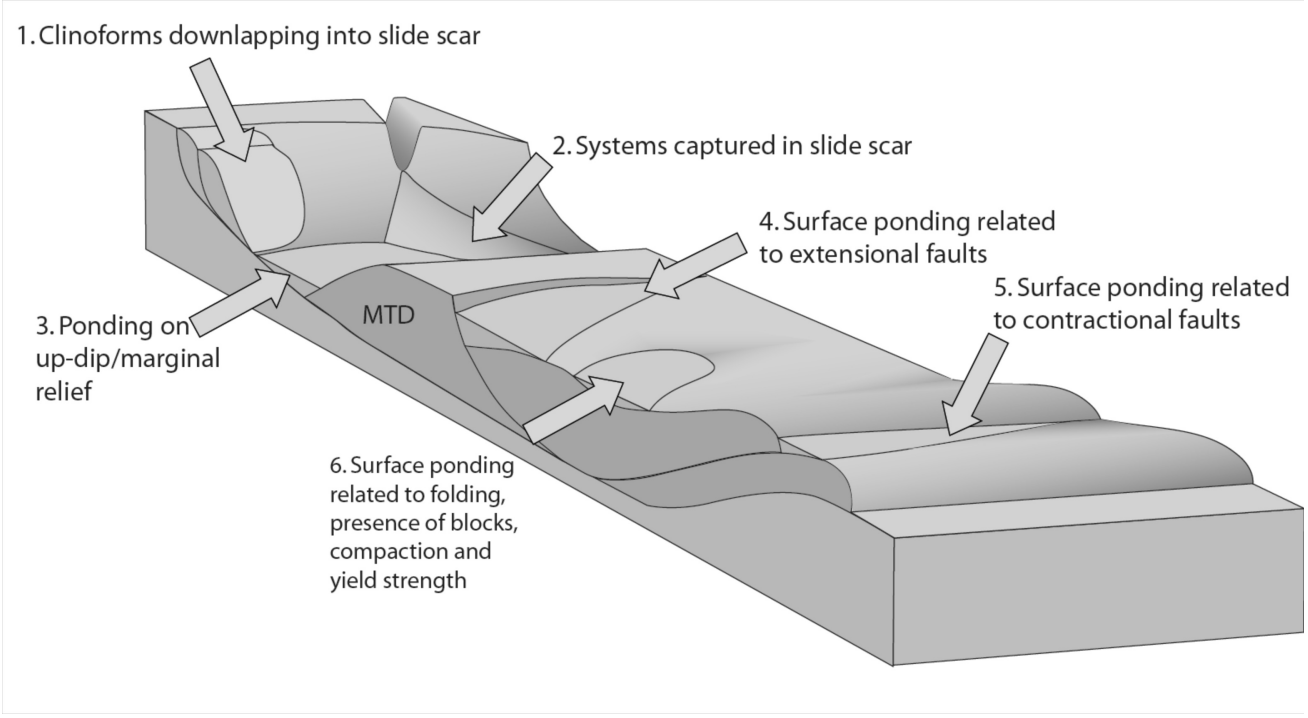

Figure 5

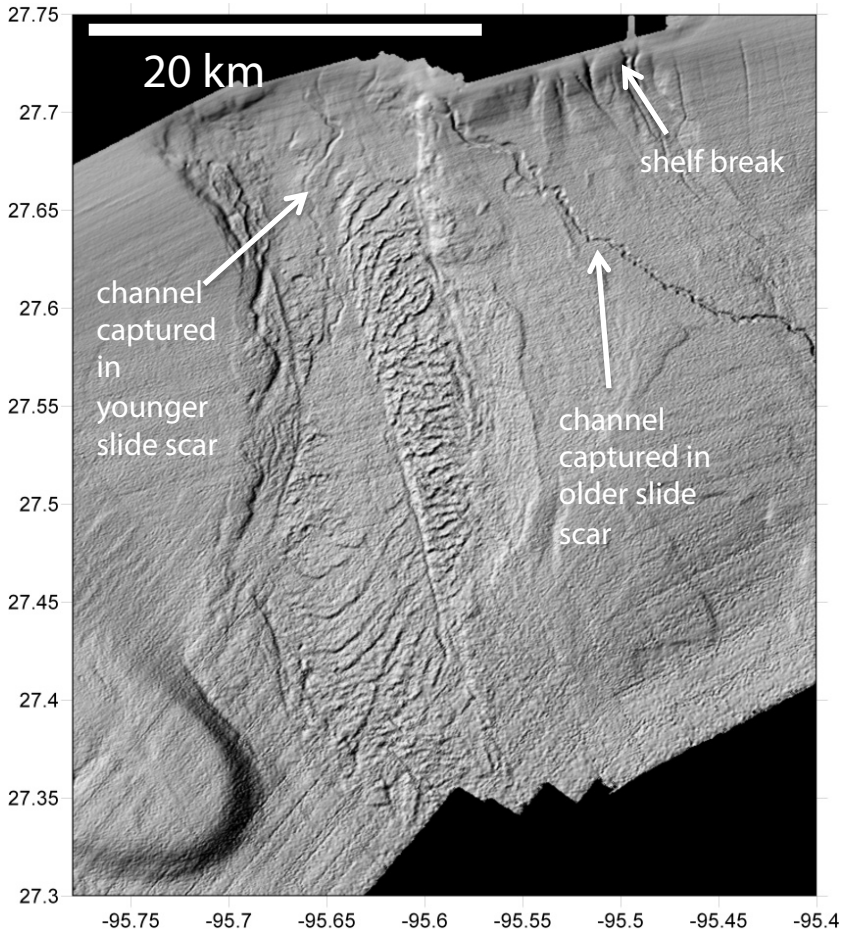

Figure 6

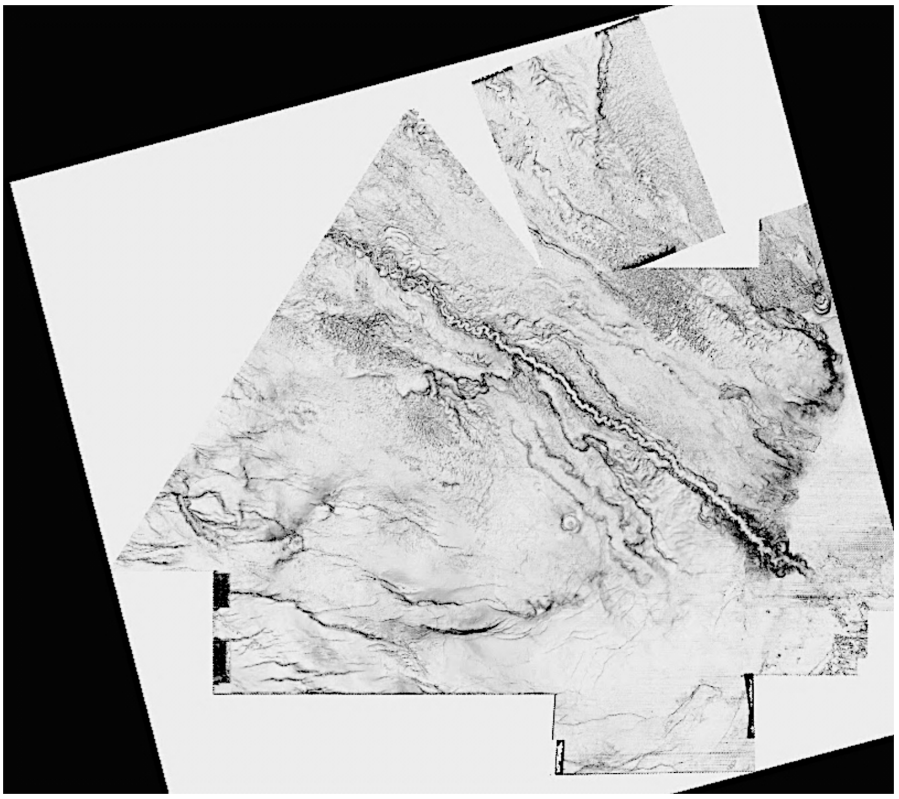

Figure 7

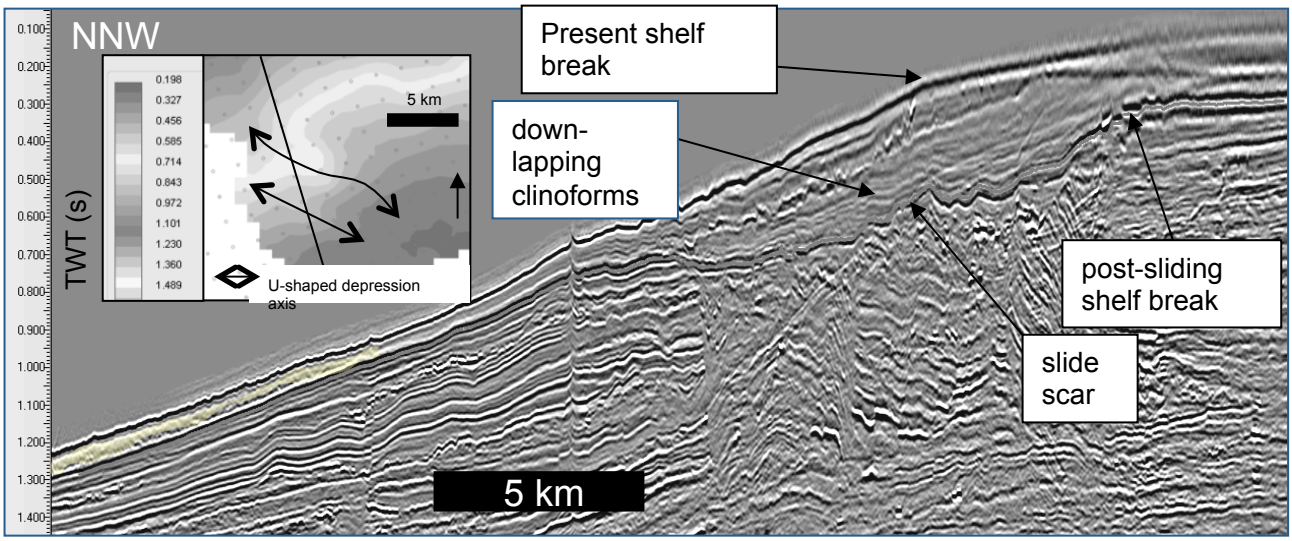

Figure 8

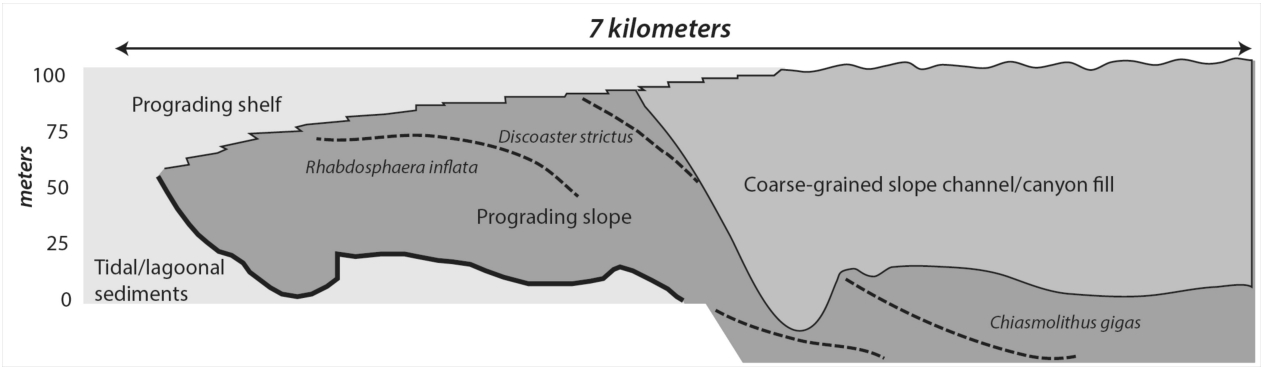

Figure 9

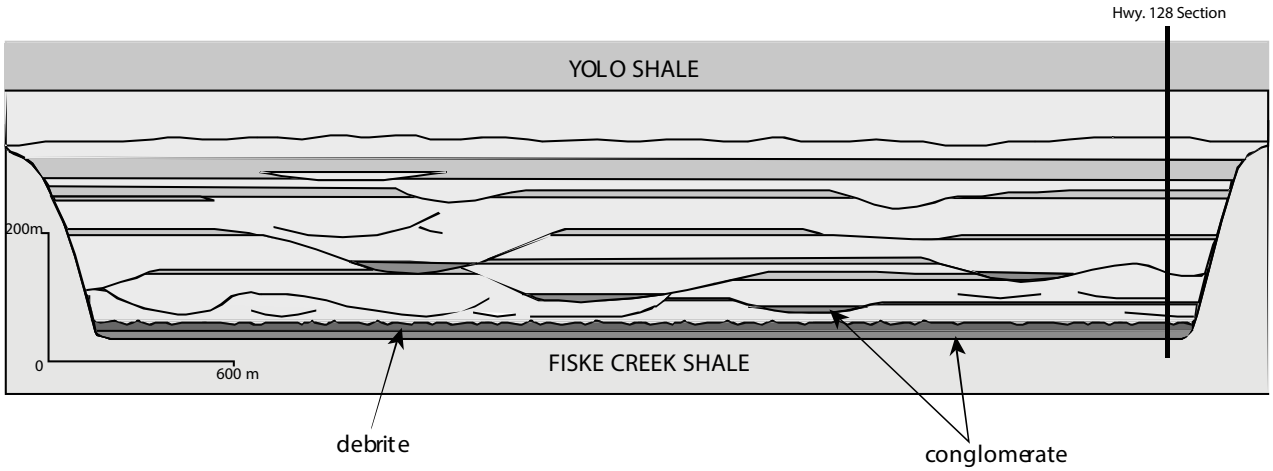

Figure 10

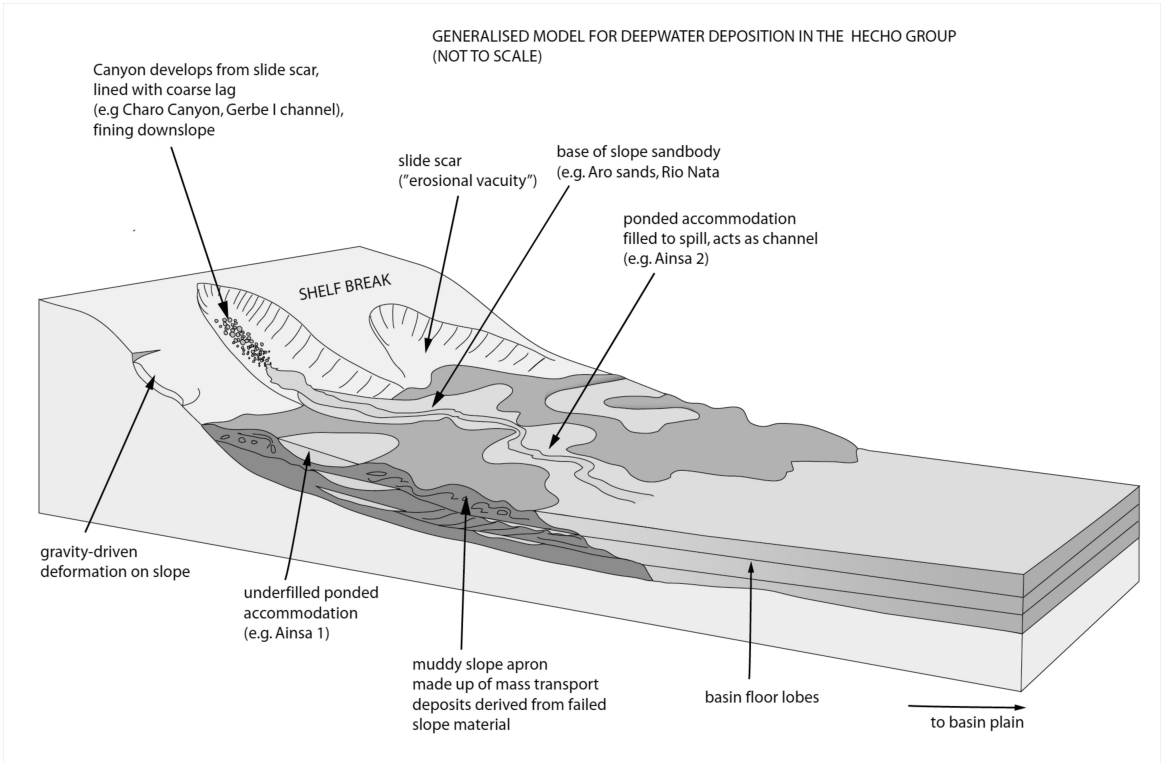

Figure 11

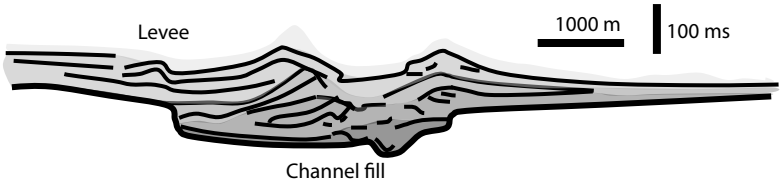

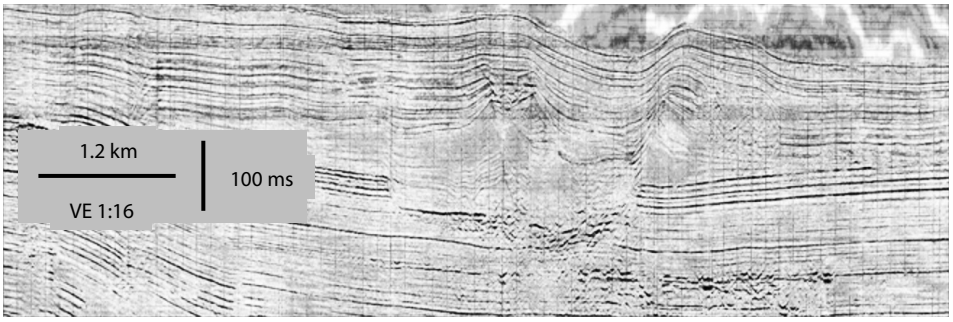

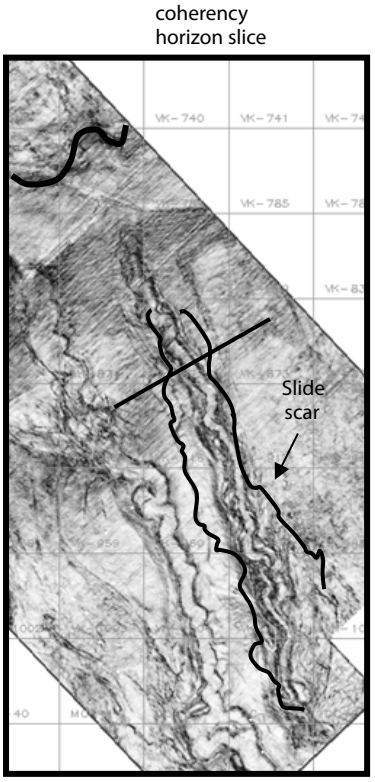

Figure 12

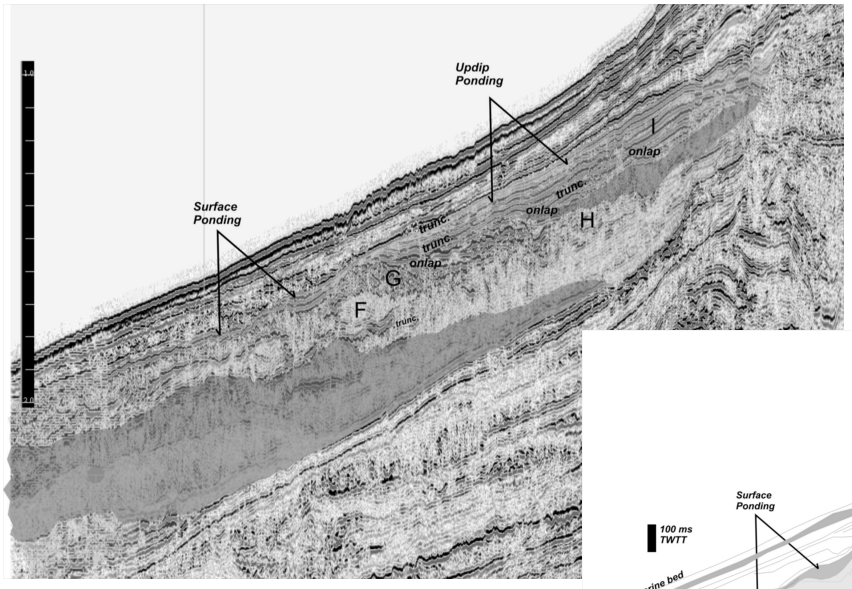

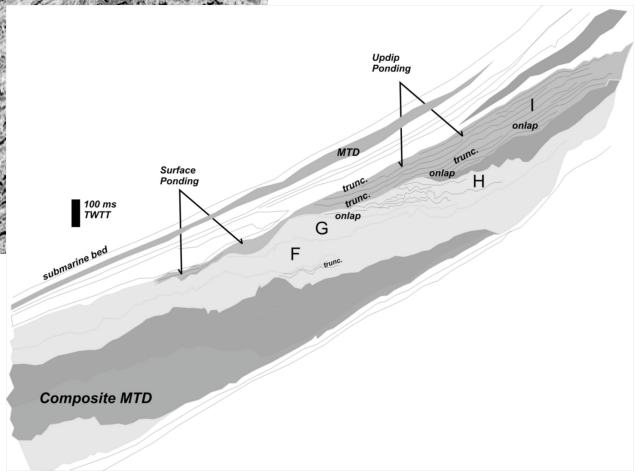

Figure 13

a

b

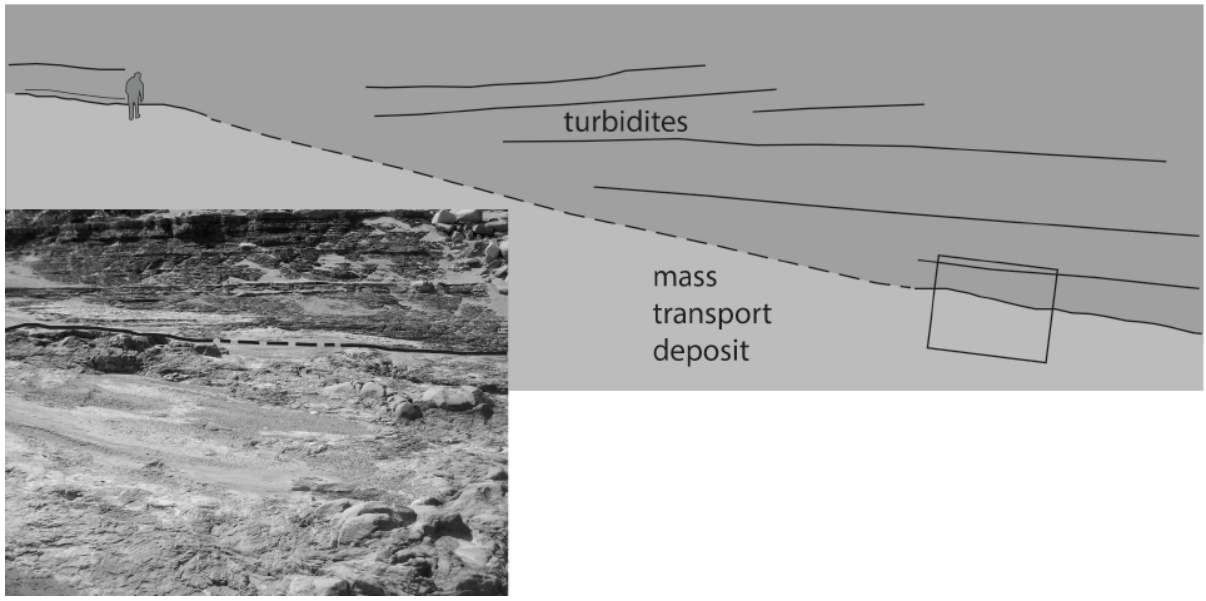

Figure 14

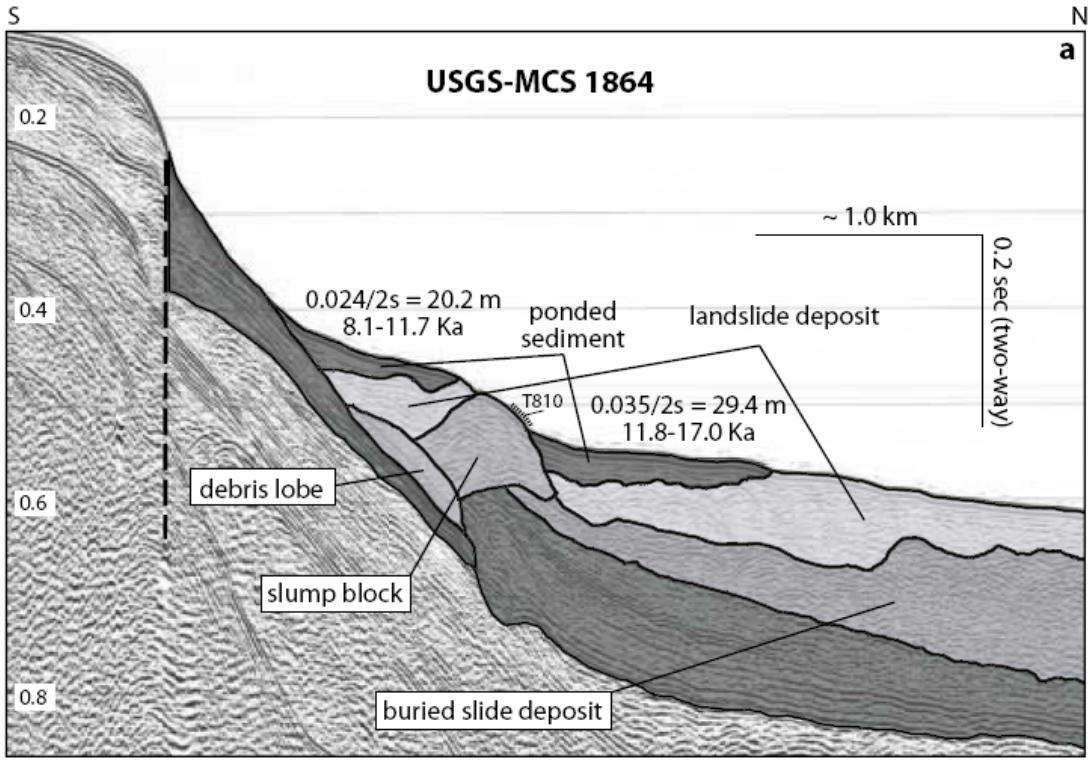
a
S
N
a
USGS-MCS 1864
0.2
0.4
0.6
0.8
~ 1.0 km
0.2 sec (two-way)
0.024/2s = 20.2 m
8.1-11.7 Ka
ponded
sediment
landslide deposit
T810
0.035/2s = 29.4 m
11.8-17.0 Ka
debris lobe
slump block
buried slide deposit

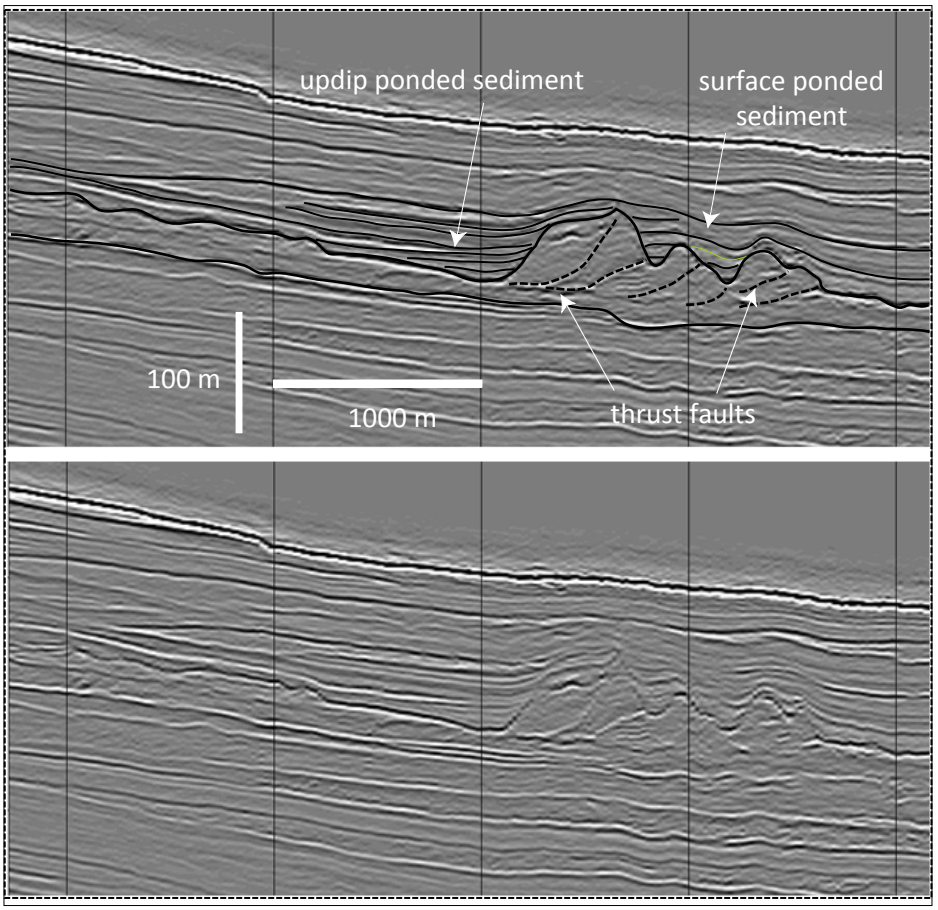
b
updip ponded sediment
surface ponded
sediment
100 m
1000 m
thrust faults

Figure 15

a

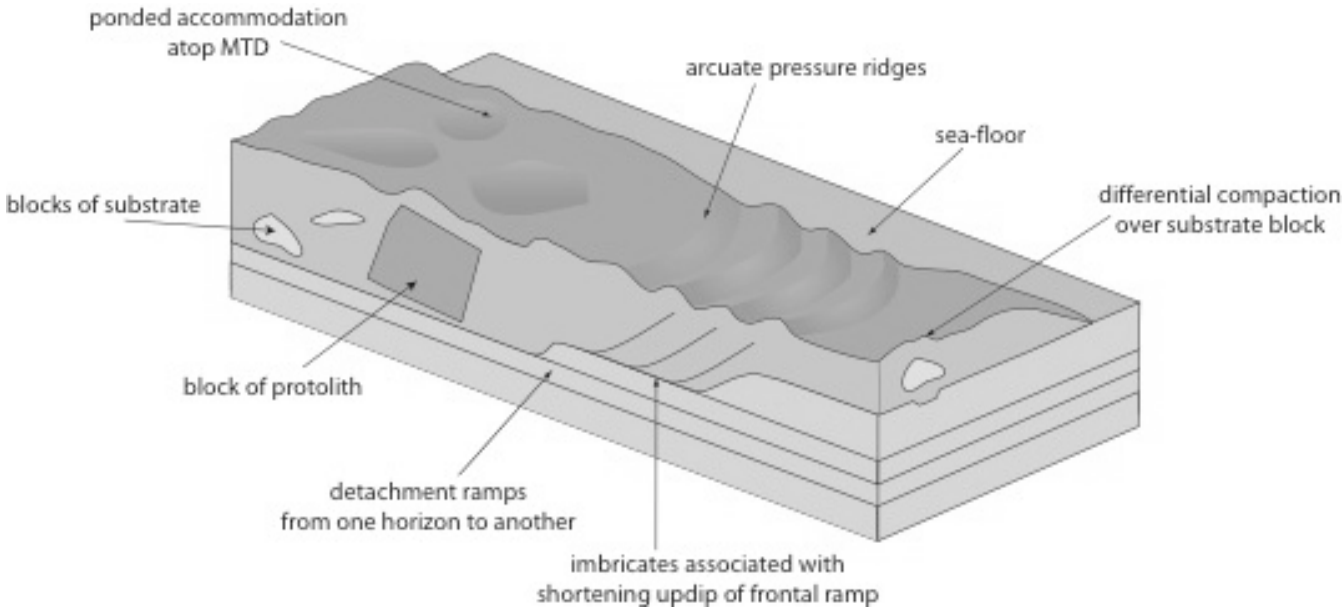

c

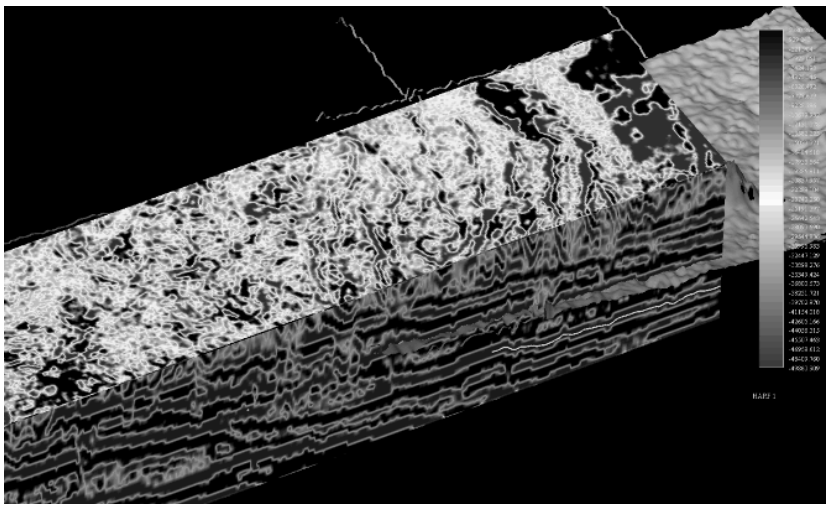

b

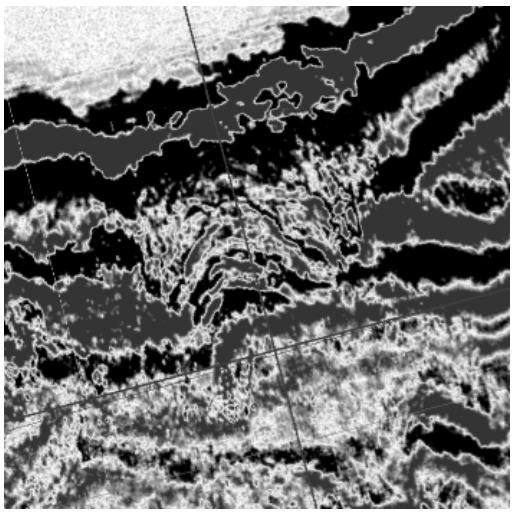

Figure 16

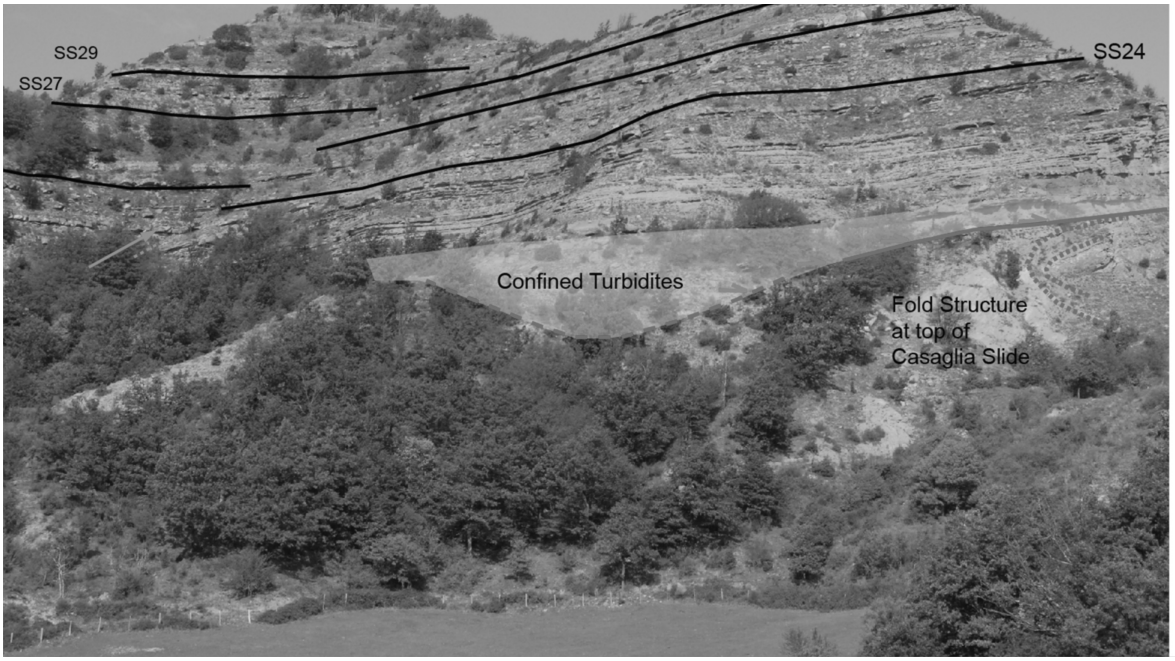

Figure 17

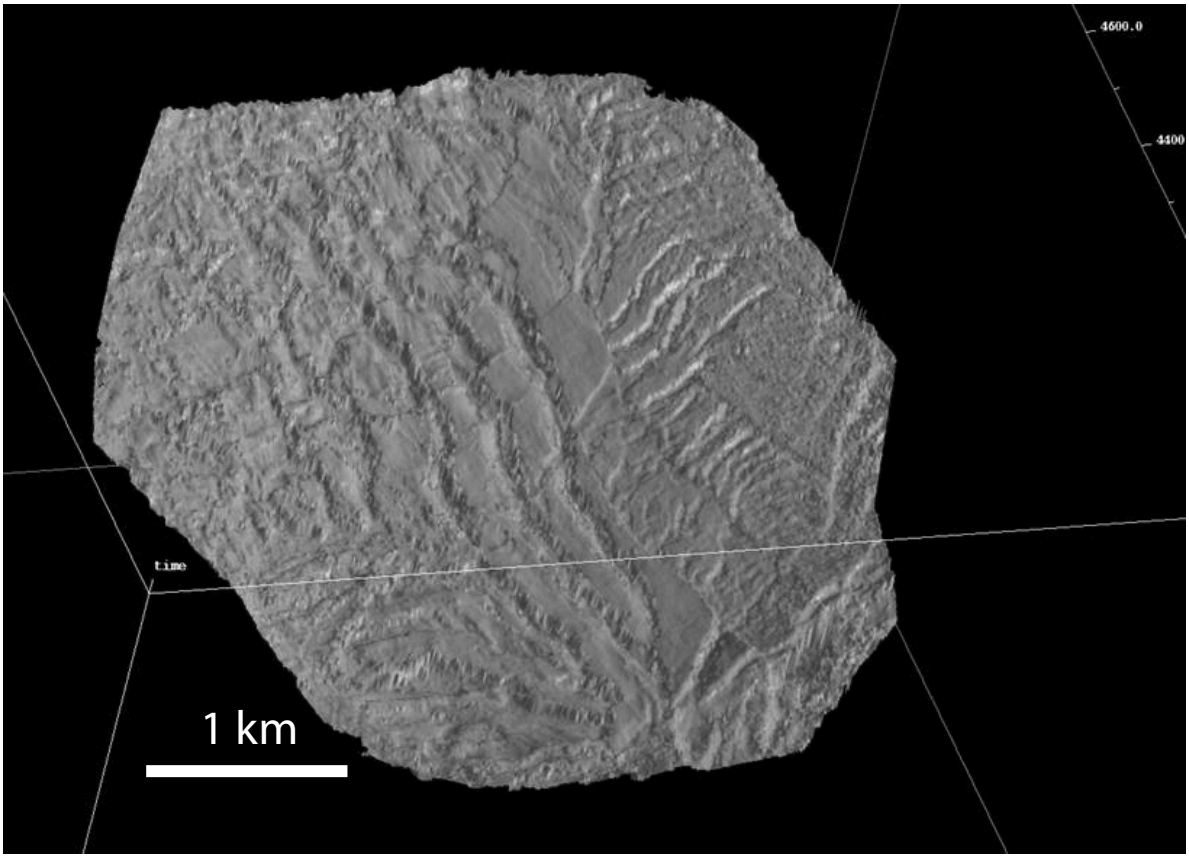

Figure 18

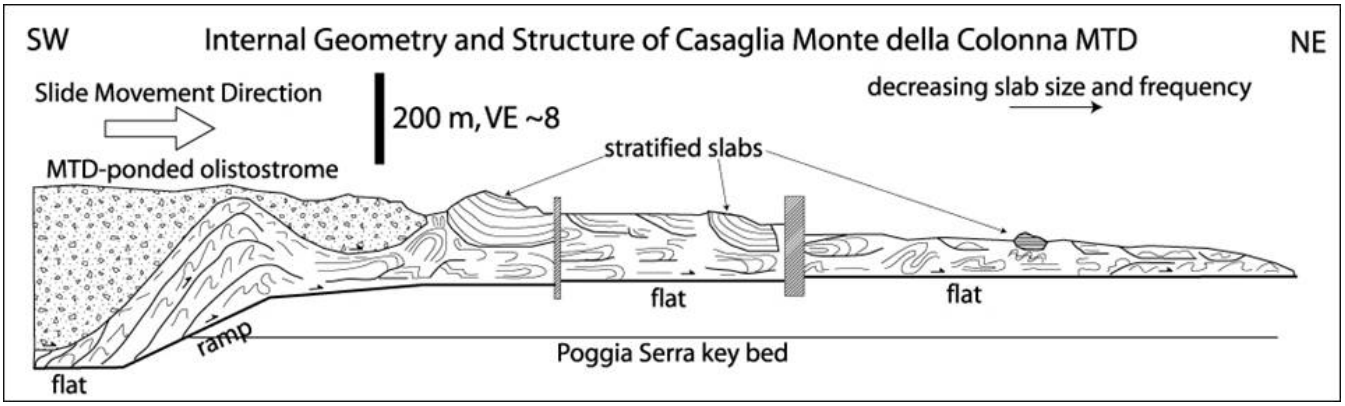

Figure 19

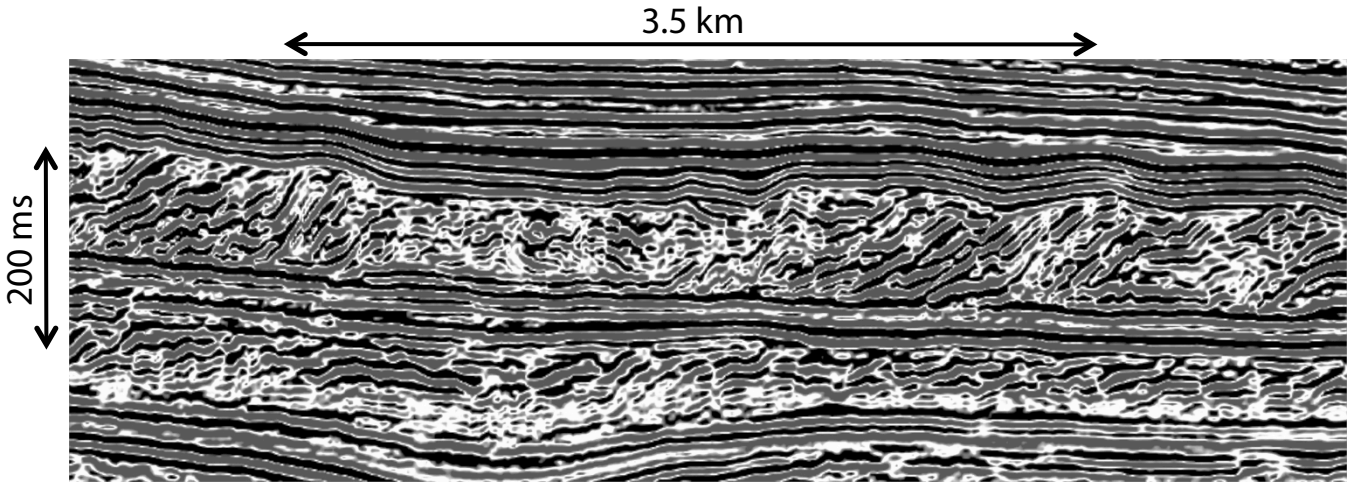

Figure 20

Figure 21

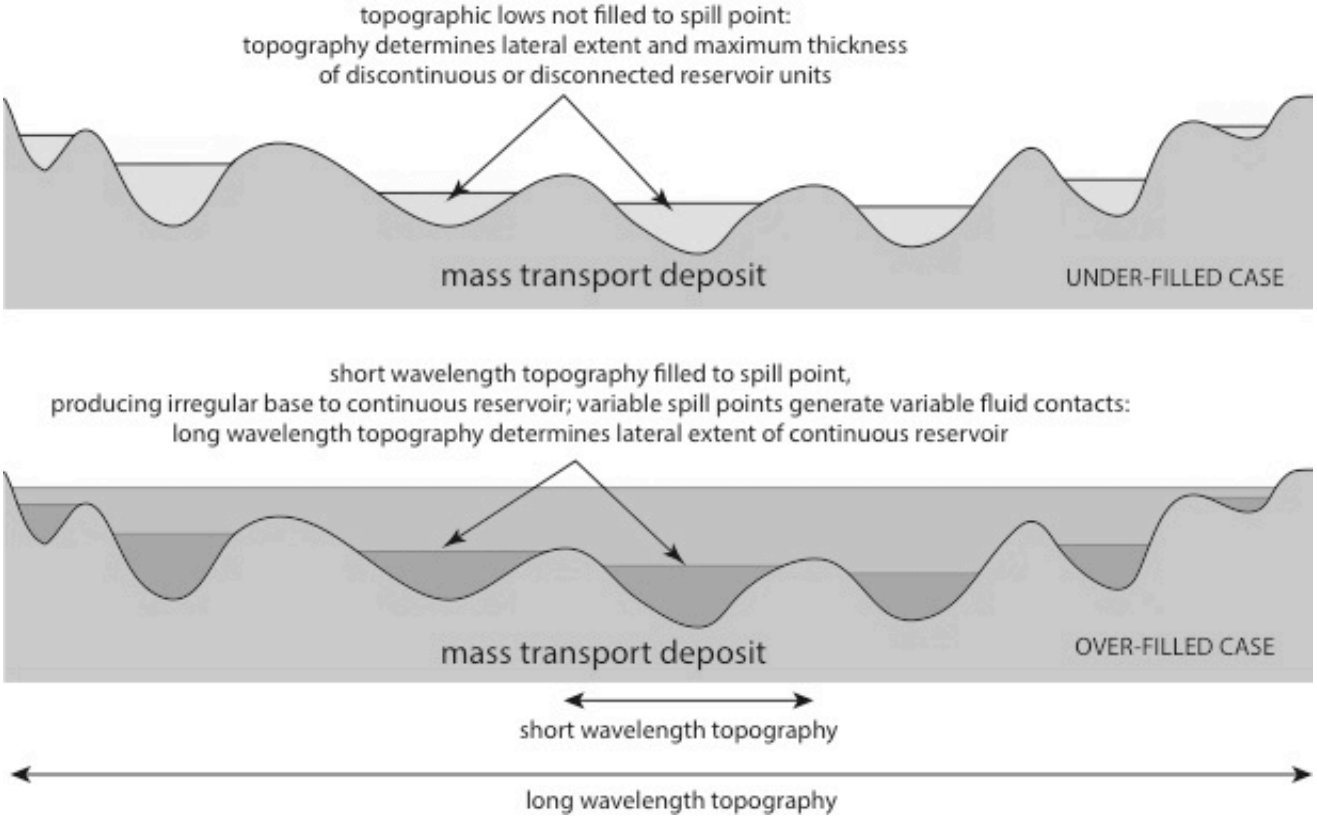

Figure 22

Ponds fill and spill (perhaps with mud bypass)

Low net-to-gross, sheeted, ponded sands; may be sequential

FLOWS PARTLY OR WHOLLY CONFINED BY TOPOGRAPHY

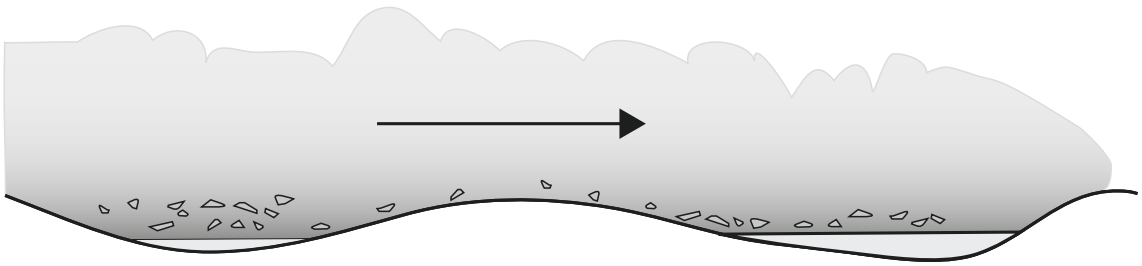

Flows over-pass from pond to pond, possibly with erosion on highs

High net-to-gross, amalgamated, ponded sands; coeval in adjacent ponds

FLOWS OUTSIZE WITH RESPECT TO TOPOGRAPHY

Figure 23

a

b

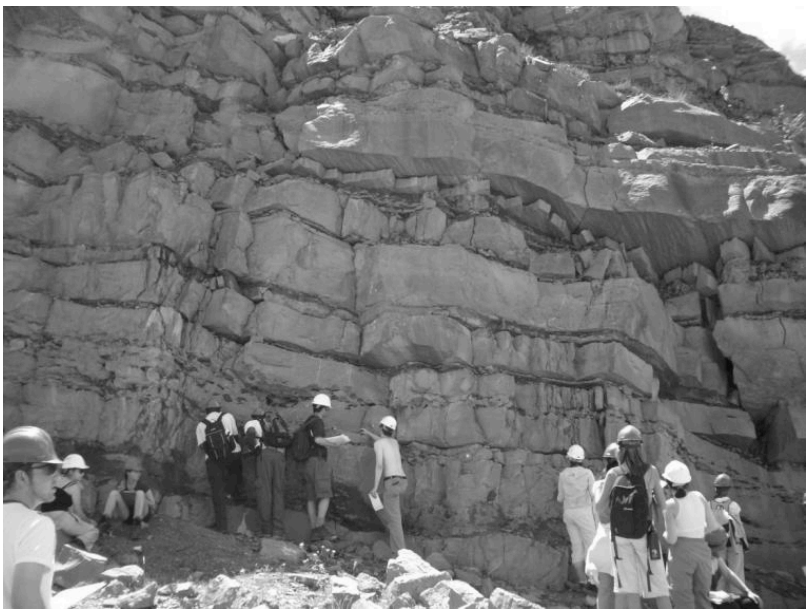

c

Figure 24

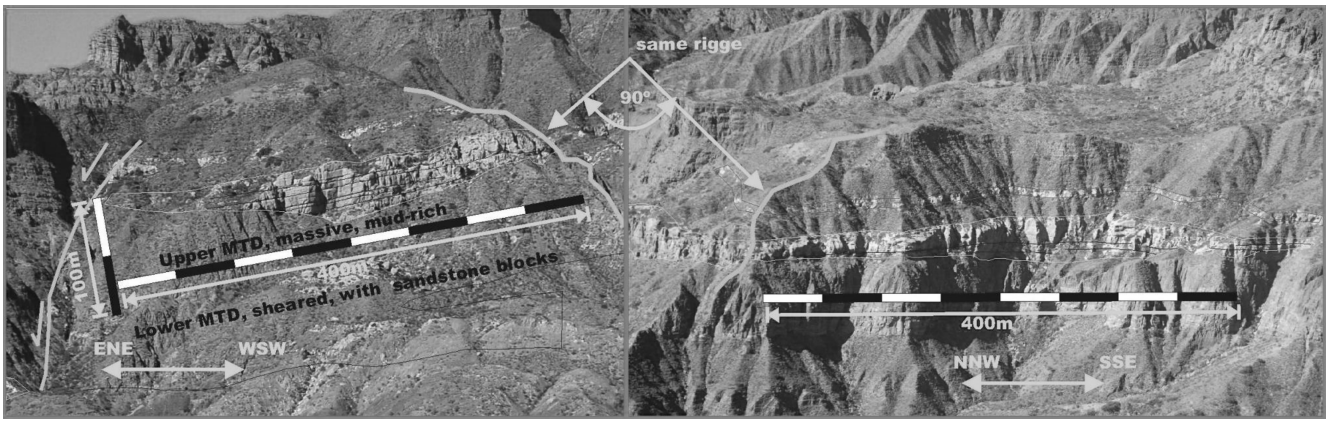

Figure 25

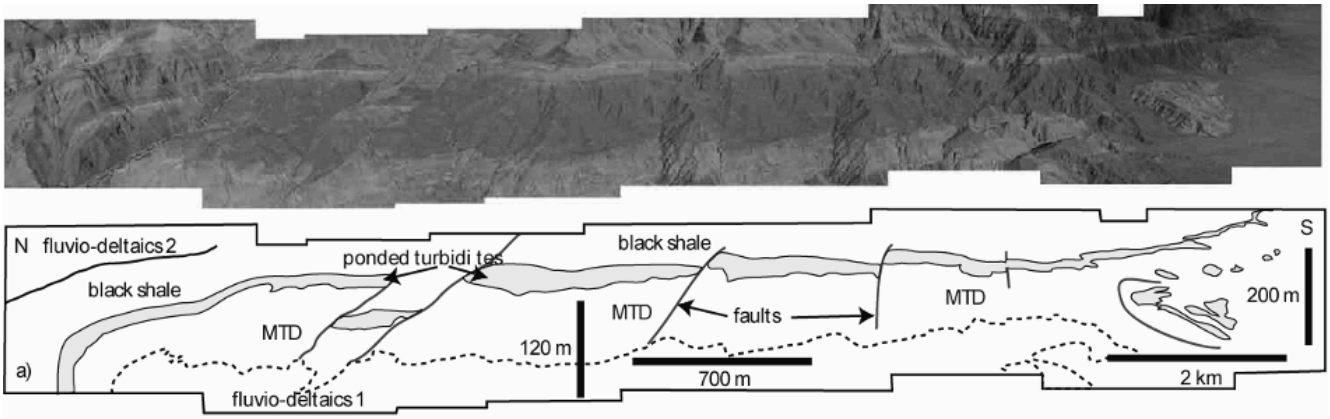

Figure 26

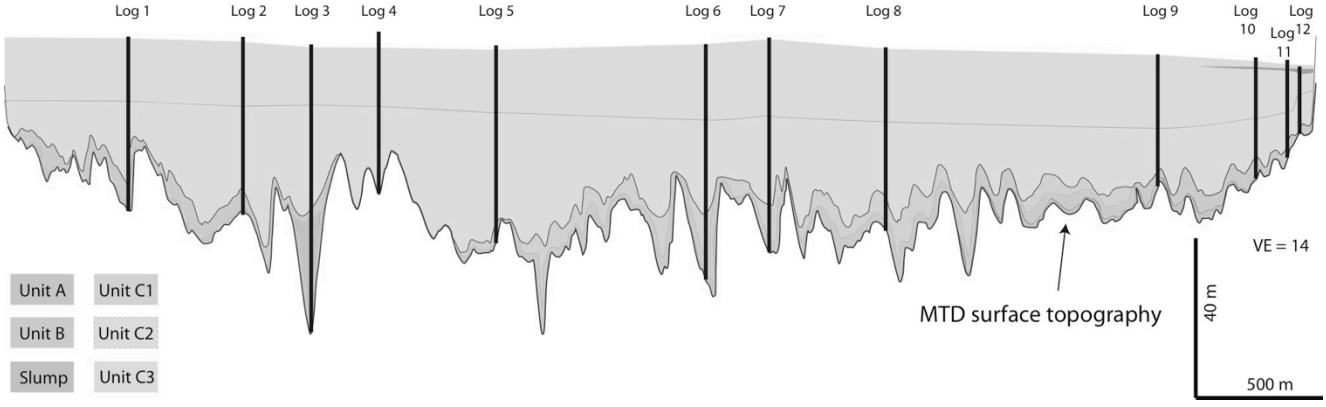

Figure 27

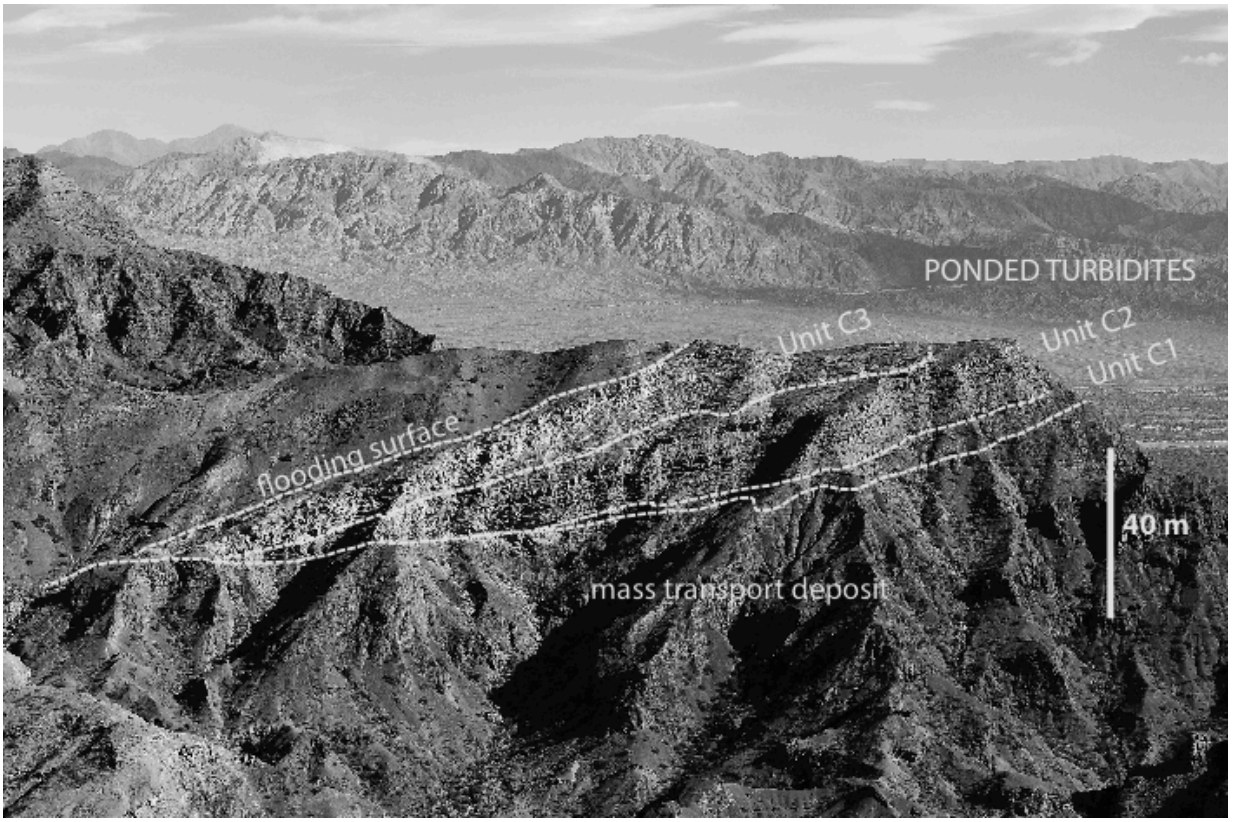
PONDED TURBIDITES
Unit C3
Unit C2
Unit C1
flooding surface
40 m
mass transport deposit